NATIONAL ADVISORY COMMITTEE FOR AERONAUTICS

TECHNICAL NOTE 2016

FLOATING CHARACTERISTICS OF RUDDERS AND ELEVATORS IN

SPINNING ATTITUDES AS DETERMINED FROM HINGE-

MOMENT-COEFFICIENT DATA WITH APPLICATION

TO PERSONAL-OWNER-TYPE AIRPLANES

By William Bihrle, Jr.

Langley Aeronautical Laboratory
Langley Air Force Base, Va.

NACA

Washington
January 1950

NATIONAL ADVISORY COMMITTEE FOR AERONAUTICS

TECHNICAL NOTE 2016

FLOATING CHARACTERISTICS OF RUDDERS AND ELEVATORS IN

SPINNING ATTITUDES AS DETERMINED FROM HINGE-

MOMENT-COEFFICIENT DATA WITH APPLICATION

TO PERSONAL-OWNER-TYPE AIRPLANES

By William Bihrle, Jr.

SUMMARY

A study was made of available rudder and elevator hinge-moment-coefficient data in order to determine the floating characteristics of various types of rudders and elevators in spinning attitudes. Some of the data were applied to specific spin attitudes obtained from tests of a model of a typical personal-owner-type airplane in the Langley 20-foot free-spinning tunnel. The results were studied with regard to obtaining spin recovery upon releasing the controls.

The plain rudder generally floated with the spin at all spinning attitudes. Of the rudders investigated, the horn-balanced rudder should be the most adaptable for obtaining desirable floating characteristics at spinning attitudes. The partial-length overhang-balanced rudder (rudder above the horizontal tail) should float near neutral for steep spins and against the spin for flatter spins. The full-length overhang-balanced rudder (a part of the rudder extending below the horizontal tail), however, may float with the spin.

Plain, overhang-balanced, and beveled-trailing-edge elevators should float in an up position in spins although the beveled-trailing-edge elevator should float closest to neutral from an up position. Horn-balanced elevators should also float in an up position. Use of large tabs deflected up should cause the elevator to float down in spinning attitudes.

INTRODUCTION

The problem of spin recovery has been extensively studied in the past from the viewpoint of obtaining recovery by rapid manual movement of the controls. References 1 and 2 present results of such

studies that may be considered applicable to personal—owner—type airplanes. Civil Air Regulations, however, require personal—owner—type airplanes to recover from spins upon releasing the controls. (See reference 3.) Some recent designs of personal—owner—type airplanes are considerably heavier than those of the past and difficulty has been encountered in complying with these Civil Air Regulations. References 1 and 2 indicate that either the rudder or elevator, depending upon the manner in which the weight is distributed in the airplane, will be the predominant control for spin recovery. In general, the rudder is moved against the spin (full left in a right spin) and the elevator is moved down for spin recovery by manual movement of the controls. Therefore, in order to obtain recovery upon releasing the controls, a type of rudder that floats against the spin and a type of elevator that floats down (from full up) appear to be the types of control surfaces required.

Although available hinge—moment—coefficient data for spinning attitudes were limited, a study of available results was made in order to determine the floating characteristics of various types of rudders and elevators in spinning attitudes. The control surfaces considered for which data at spinning attitudes were available (references 4 to 8) included a plain and an overhang—balanced rudder and a plain, an overhang—balanced, and a beveled—trailing—edge elevator. A horn—balanced rudder and a horn—balanced elevator were also considered although data (references 9 and 10) were not available for these types of control surfaces at spinning attitudes. Some of the data have been applied to specific spin attitudes obtained on a model of a typical personal—owner—type airplane that has been tested in the Langley 20—foot free—spinning tunnel.

SYMBOLS

S wing area, square feet

b wing span, feet

c' mean aerodynamic chord of wing, feet

x/c' ratio of distance of center of gravity rearward of
             leading edge of mean aerodynamic chord to mean
             aerodynamic chord

z/c' — ratio of distance between center of gravity and thrust line to mean aerodynamic chord (positive when center of gravity is below thrust line)

m — mass of airplane, slugs

ρ — air density, slugs per cubic foot

V — full-scale true rate of descent or free-stream velocity, feet per second

q — dynamic pressure, pounds per square foot $\left(\frac{1}{2}\rho V^2\right)$

μ — airplane relative-density coefficient $(m/\rho S b)$

I_X, I_Y, I_Z — moments of inertia about X-, Y-, and Z-body axes, respectively, slug-feet square

$\dfrac{I_X - I_Y}{mb^2}$ — inertia yawing-moment parameter

$\dfrac{I_Y - I_Z}{mb^2}$ — inertia rolling-moment parameter

$\dfrac{I_Z - I_X}{mb^2}$ — inertia pitching-moment parameter

α — angle between vertical and thrust axis (approx. equal to absolute angle of attack at plane of symmetry), degrees

R_s — spin radius, distance from spin axis to center of gravity, feet

Ω — full-scale angular velocity about spin axis, radians per second

β_t — approximate angle of sideslip at tail (angle between relative wind and plane of symmetry at tail, positive when relative wind comes from right of plane of symmetry at tail), degrees

δ_r — rudder deflection with respect to fin (positive when trailing edge is deflected to left), degrees

δ_{r_t} — total rudder deflection from stop to stop

δ_e elevator deflection with respect to stabilizer (positive when trailing edge is deflected down), degrees

δ_{t_e} elevator tab deflection with respect to elevator, degrees

l_r total rudder-pedal travel, from full forward to full rearward, feet

b_r rudder height along hinge axis, feet

$\bar{c}_r$ root-mean-square chord of rudder (rearward of hinge line), feet

b_e elevator span (along hinge axis), feet

$\bar{c}_e$ root-mean-square chord of elevator (rearward of hinge line), feet

c mean geometric chord of tail, feet

c_e mean geometric chord of elevator, feet

C_{h_r} rudder hinge-moment coefficient $\left(H_r/qb_r\bar{c}_r^2\right)$

C_{h_e} elevator hinge-moment coefficient $\left(H_e/qb_e\bar{c}_e^2\right)$

H_r rudder hinge moment (positive when it tends to deflect rudder to left), foot-pounds

H_e elevator hinge moment (positive when it tends to deflect elevator trailing edge down), foot-pounds

F rudder-pedal force (positive when push force is on right rudder pedal), pounds $\left(H_r \dfrac{\pi}{180} \dfrac{\delta_{r_t}}{l_r}\right)$

α_s angle of attack of control surface, degrees

C_{h_δ} rate of change of hinge—moment coefficient with control—surface deflection for constant control—surface angle of attack

$C_{h_{\alpha_s}}$ rate of change of hinge—moment coefficient with control—surface angle of attack for constant control—surface deflection

SCOPE AND LIMITATIONS OF INVESTIGATION

The data studied were obtained from references 4 to 10 and were for plain, overhang—balanced, and horn—balanced rudders and plain, overhang—balanced, horn—balanced, and beveled—trailing—edge elevators. Table I indicates the types of control surfaces studied, the ranges of angles of attack and sideslip and the control deflections considered, and the references from which the data presented herein were obtained. The data presented were taken from the references for unsealed control surfaces, except where otherwise noted. This selection was made primarily because most personal—owner—type airplanes use unsealed surfaces.

The data for the plain rudder were analyzed for only the two most typical combinations of the vertical and horizontal tails presented in reference 4, that is, for the horizontal tail in a low and in a high position, longitudinally alined with the vertical tail. Results presented for a balanced rudder with a 27.9—percent—area overhang were obtained from reference 5; results for a balanced rudder with a 43.5—percent—area overhang, available from reference 6 for only two angles of attack and two rudder deflections, are not presented quantitatively but are discussed briefly. The data for a balanced rudder with a 14.5—percent—area horn (reference 9) were available only for the vertical tail without the presence of the horizontal tail at 0° angle of attack and are for a surface with an unshielded horn and with a sealed gap. Sketches of the vertical tails for which numerical data are presented herein are shown in figures 1, 2, and 3.

The results presented herein are for zero sideslip but a discussion of the effects of sideslip, based on the limited data available, is also included. The data presented from reference 7 are for a plain elevator and a blunt—nose balanced elevator with a 35—percent—chord overhang. Reference is also made to results from reference 7 for a blunt—nose

balanced elevator with a 50-percent-chord overhang although no quanti-
tative data are repeated herein. Data from reference 5 for a balanced
elevator with a 31.8-percent-area overhang were analyzed for the
effects of tab size on the floating characteristics of this elevator.
Beveled-trailing-edge-elevator results of reference 8 are presented
herein only for a 10-percent-chord bevel. Results from reference 6
for a balanced elevator with a 48-percent-area overhang and from
reference 10 for a horn-balanced elevator are mentioned briefly,
but numerical results are not presented. Sketches of the horizontal
tails for which numerical data are presented herein are shown in
figures 4 and 5.

The data obtained from references 4, 5, and 6 were for the control
surface in the presence of a complete tail combination; whereas the
data from the remaining references were for isolated tail surfaces.
The effect of fuselage interference on the rudder and elevator floating
characteristics is not known because comparative data do not exist,
and for this investigation, therefore, results for surfaces that
were tested in the presence of a fuselage were compared in some
instances with those that were not. Also, all the available hinge-
moment-coefficient data were obtained with static models and the
effects of friction and of centrifugal force have been neglected. A
preliminary study, however, has indicated that, for the average
personal-owner-type airplane, the effects of centrifugal force on
the rudder do not change the comparative floating tendencies of the
rudders presented herein.

Hinge-moment characteristics of various types of control surfaces
at normal flight attitudes are presented in reference 11.

METHODS OF ANALYSIS

In order to determine the general floating characteristics of the
various control surfaces through ranges of angle of attack and angle of
sideslip, cross plots of hinge-moment coefficient against control
deflection δ_r and δ_e have been prepared from the data of the refer-
ences. The floating angles can be readily determined, since they are
the control deflections at which the hinge-moment coefficient is equal
to zero. In this analysis, the angles of sideslip are equal in magni-
tude but opposite in sign to the angles of yaw used in the references.

The floating characteristics of the control surfaces for specific
spinning conditions obtained on a model of a typical personal-owner-
type airplane having different tail configurations were obtained by
interpolation of the general hinge-moment-coefficient data. The
specific application was made to show the method of applying the

general data in determining the floating characteristics of rudders
at actual spin conditions, for a range of spin conditions that are
probable for personal–owner–type airplanes. The general data applied
to these spin conditions were for the plain rudder and for the
27.9–percent–overhang–balanced rudder. The hinge–moment–coefficient
data for the horizontal tail in the low and in the high positions
on the plain rudder were interpolated so that the vertical position
of the horizontal tail used for the hinge–moment–coefficient data
simulated the vertical position of the horizontal tail on the spinning
model. This method of application was not possible for the
27.9–percent–overhang–balanced rudder because the general hinge–
moment–coefficient data were available for only one horizontal–tail
position. Some typical spinning attitudes assumed by the free–spinning
model were used to determine the floating characteristics of an
overhang–balanced rudder. A comparison was also made between the
plain and overhang–balanced rudder for specific spinning attitudes
assumed by the spinning model for those conditions for which the
dynamic model had a tail configuration similar to that for the
27.9–percent overhang balance.

Photographs of the spinning model are shown in figure 6 and the
dimensional and mass characteristics of the model in terms of full–
scale values are presented in table II. Drawings of the various tail
assemblies tested on the model are shown in figure 7. The free–spinning
model tests were performed in the manner explained in reference 12,
except that the launching technique has been changed from launching
by a spindle to launching by hand. The spin data presented were
obtained and converted to full–scale values by the methods also
described in reference 12.

In addition to determining the floating characteristics of the
plain rudder at specific spinning attitudes, calculations were made to
determine the rudder–pedal force that would·be required to hold the
rudder at neutral. The forces were calculated by the method presented
in reference 4 and were based on an assumed total rudder–pedal travel,
from full forward to full rearward, of 5 inches (0.417 ft) and a rudder
deflection range of 60°. These values are approximate averages for
personal–owner–type airplanes and therefore the value $\dfrac{\pi}{180}\dfrac{\delta_{rt}}{l_r}$ used
was 2.51.

PRESENTATION OF RESULTS

The general hinge–moment characteristics of a plain rudder are
presented in figures 8 and 9 for the tail combinations having the
horizontal tail in the low and high center positions, respectively.
The general hinge–moment characteristics of the 27.9–percent–
overhang–balanced rudder are presented in figure 10 and those for the

14.5-percent-horn-balanced rudder, in figure 11. The hinge-moment characteristics of the various rudders are presented for various angles of attack and sideslip in the form of curves of hinge-moment-coefficient plotted against control deflection.

The spinning conditions obtained for various control settings on the model of the typical personal-owner-type airplane having different tail configurations are presented in table III. The angles of-attack and sideslip, rate of rotation, vertical rate of descent, and spin radius are presented.

Hinge-moment characteristics at specific spinning attitudes are presented in figures 12 to 14 for the plain rudder and in figure 15 for the 27.9-percent-overhang-balanced rudder. A comparison of the floating tendencies of the plain and 27.9-percent-overhang-balanced rudders at some specific spin attitudes is indicated in figure 16. The floating angles obtained from figures 12 to 16 and the rudder-pedal forces required to hold the plain rudder at neutral are also listed in table III for each specific spinning condition.

The general hinge-moment characteristics of the plain, 35-percent-overhang-balanced, and beveled-trailing-edge elevators are shown in figure 17. The hinge-moment characteristics of the 31.8-percent-overhang-balanced elevator and the effects of tab deflection on its hinge-moment characteristics are presented in figure 18.

RESULTS AND DISCUSSION

Studies have indicated that deflections of the rudder and elevator are the predominant control-surface movements required for spin recovery, the use of either or both depending on the weight distribution within the airplane. (See references 1 and 2.) Insofar as existing studies are based on full manual movement of the control surfaces, the amount of control-surface movement necessary for satisfactory spin recovery is not known, although the amount would probably vary with the designs and loadings of the airplanes. In order to comply with the Civil Air Regulations (reference 3), which require spin recovery with controls free, the floating characteristics of the rudder and elevator surfaces for any given design would have to be such that the control surfaces would float to the position required for obtaining satisfactory recovery for the worst loading condition. Inasmuch as the direction but not the magnitude of control-surface travel necessary for recovery is known, the assumption is made that, for a given tail design, the type of rudder that floats farthest against the spin and the type of elevator that floats farthest down

would be the types of control surfaces desirable for spin recovery by released controls.

Rudder Floating Characteristics

The floating characteristics of rudders depend primarily on the aerodynamic hinge-moment coefficients of the rudder surface, which depend on the sideslip that exists at the tail in the spin (the angle of attack of the vertical surface) and upon the deflection of the surface. The angle of attack of the spin also influences rudder hinge-moment characteristics, mainly because it determines the extent to which the horizontal tail will shield the vertical tail. The wake of the horizontal tail produces a shielding or blanketing effect and the part of the rudder in the wake becomes relatively ineffective. (See references 4 and 5.) The part of the rudder that will be encompassed by the wake depends on the position of the horizontal tail in relation to the vertical tail. The wake generally encompasses only the lower and rearward sections of the rudder at low angles of attack and moves upward and forward as the angle of attack increases, the front of the wake boundary pivoting about the leading edge of the stabilizer. (See fig. 19.) Sideslip at the tail also influences to some degree the amount of shielding obtained. The shielding generally tends to become smaller as the outward sideslip at the tail increases. Because high angles of attack result in the shielding of the rudder by the horizontal tail and because high angles of sideslip at the tail may result in the stalling of the vertical surfaces, the variations of hinge-moment coefficient with α_s and δ_r are not linear and, therefore, the values of $C_{h_{\alpha_s}}$ and C_{h_δ} obtained in normal flight or in spin attitudes cannot be used to calculate the floating angles at spin attitudes.

The subsequent discussion is about the floating characteristics of various types of rudders with consideration of the effects of the factors just discussed.

Plain rudders.- The curves of rudder hinge-moment coefficient plotted against rudder deflection for the tail combination with the horizontal tail in the low position (fig. 8) show changes in the general slopes with increasing angle of attack. At spinning angles of attack of 10° to 30° well-defined floating angles are obtained; whereas at higher angles of attack the floating angles are generally not well defined primarily because of the shielding of the vertical tail by the horizontal tail. At low spinning angles of attack, the floating angle of the rudder is a function of sideslip. The rudder

floats progressively more with the spin (right in a right spin) as
the outward sideslip at the tail increases (the relative wind coming
from the left side of the plane of symmetry in a right spin).
Unpublished results of numerous models tested in the Langley 20-foot
free-spinning tunnel indicate that airplanes usually spin with
outward sideslip at the tail. The results for the typical personal-
owner-type airplane (table III) show a 1.7° to 32.8° variation in
outward sideslip at the tail.

As the angle of attack increases above 30°, the hinge-moment-
coefficient curves become erratic and the coefficient values become
small; these conditions indicate that the rudder becomes almost
completely shielded. The indicated floating characteristics are
irregular and inconclusive. Prediction of the floating angles for
such highly shielded conditions may, however, not be necessary, because
satisfactory recoveries would probably be difficult or impossible to
obtain even by manual operation of the rudder. At angles of outward
sideslip of 30° for angles of attack of 40° or more, the rudder
becomes unshielded and floats full with the spin.

The floating characteristics for the tail combination with the
horizontal tail in the high position (fig. 9) are similar to those
obtained with the horizontal tail in the low position (fig. 8). When
the horizontal tail is in the high position, however, the rudder does
not become shielded even at high angles of attack for moderate values
of outward sideslip.

Figures 8 and 9 indicate that the floating characteristics of a
plain rudder in a spin are such that the rudder assumes a deflection
with the spin and that this deflection progressively increases with
increasing outward sideslip. In general, in a steep spin small outward
sideslip is present at the tail and in a flat spin large outward
sideslip is present; therefore, a plain rudder on a personal airplane
that is in a flat spin will probably float full with the spin. For a
specific tail combination, the essential effect of angle of attack on
rudder floating angles is determined by the amount of rudder shielding
resulting at that angle of attack.

Overhang-balanced rudders.- The curves of hinge-moment coefficient
plotted against rudder deflection for the 27.9-percent-overhang-
balanced rudder (fig. 10) show changes in the general slopes of the
curves with changes in airplane angle of attack. The fact that these
changes in slope are similar to those obtained for the plain rudders
indicates effects of shielding on the overhang-balanced rudder similar
to those on the plain rudder. The C_{h_δ} values for the small angles of

attack are negative, and the absolute values of these slopes

progressively decrease until they become positive (unstable) above an angle of attack of 38°. As the angle of attack increases, the shielding effect of the horizontal tail results in an increased ratio of unshielded balance area to unshielded rudder area. This increase results in the change in slope previously mentioned and indicates that beyond an angle of attack of 38° the unshielded part of the rudder has become overbalanced.

Figure 10 indicates that the floating characteristics of the 27.9-percent-overhang-balanced rudder are not appreciably affected by sideslip at the steeper-spin angles of attack (28° or less). This fact indicates that for this control surface, the hinge-moment coefficients were not appreciably affected by angle of attack of the surface (the angle of attack of the vertical tail is the sideslip angle). In other words, the normally considered $C_{h_{\alpha_s}}$ was approximately zero. For the flatter-spin angles of attack when the rudder is overbalanced, the results indicate that the rudder may float either full with or full against the spin, the direction depending on whether the hinge-moment coefficient existing at the time of rudder release is negative or positive. As indicated in figure 10, outward sideslip of 20° generally resulted in a floating angle full against the spin; whereas outward sideslip of only 10° resulted in a floating angle full with the spin.

The results of limited tests for the 43.5-percent-overhang-balanced rudder (reference 6) show probable floating characteristics that differ somewhat from those for the 27.9-percent-overhang-balanced rudder. The span of the 27.9-percent-balanced rudder terminated at the top of the fuselage and above the horizontal tail (partial-length rudder); whereas the span of the 43.5-percent-balanced rudder extended to the bottom of the fuselage and below the horizontal tail (full-length rudder). At the low angle of attack for which data are available (20°), $C_{h_{\alpha_s}}$ is negative and not zero as it is for the case of the partial-length rudder. This difference would cause the full-length overhang-balanced rudder to float with the spin, inasmuch as C_{h_δ} is also negative. Similar results may be expected at higher angles of attack because the data at the higher angle of attack (50°) show that $C_{h_{\alpha_s}}$ is still negative. The most favorable floating characteristics therefore can probably be obtained from overhang-balanced rudders when they are partial length, and the least favorable when they are full length and have a high horizontal-tail position.

A comparison of the results in figures 10(a), 10(b), and 10(c) shows that deflecting the elevators did not appreciably affect the rudder hinge—moment coefficients or the floating characteristics of the partial—length 27.9—percent—overhang—balanced rudder for angles of attack from 18° to 68°. The results of the tail configuration with a full—length 43.5—percent—overhang—balanced rudder (reference 6) also indicated that the rudder hinge—moment coefficients were not appreciably affected by elevator deflection for angles of sideslip and rudder deflections of like signs when the angle of attack was approximately 20°, but at an angle of attack of 50°, an effect, although inconsistent, was indicated. An effect of elevator deflection would therefore be expected only when accompanied by a change in the shielding of the rudder.

Horn—balanced rudders.— The hinge—moment—coefficient data of the horn—balanced rudder (fig. 11) obtained from reference 9 were for zero angle of attack and no horizontal tail. For this unshielded rudder condition, negative values of C_{h_δ} and positive values of $C_{h_{\alpha_s}}$ were obtained. Although the magnitude of the values of C_{h_δ} and $C_{h_{\alpha_s}}$ obtained were considered undesirable for normal flight, as indicated in reference 9, the hinge—moment characteristics are considered to be indicative of what would be obtained on a rudder which is satisfactory for normal flight when it became shielded in spinning attitudes. A comparison of the results of figure 11 with the data for the overhang—balanced rudder at the low angles of attack (fig. 10) indicates that the horn—balanced rudder would have more favorable floating characteristics, with regard to spin recovery, in that it would generally tend to float more against the spin. This more favorable floating characteristic occurs over a limited range of—angles of attack of the surface when the horn—balanced rudder has a positive value of $C_{h_{\alpha_s}}$ and a negative value of C_{h_δ}. The floating characteristics of the horn—balanced rudder however would probably be superior to the overhang—balanced surface through the entire spinning angle—of—attack range if the rudder were in the presence of a horizontal tail. As in the case for the overhang—balanced rudder, the wake of the horizontal tail would shield the horn—balanced rudder so that the ratio of unshielded balance area to unshielded rudder area would increase as the angle of attack increased. This effect is indicated in figure 19. For the case of the horn balance, the balance area may be completely unshielded until very flat spins are obtained and, therefore, a much larger ratio of unshielded balance area to unshielded rudder area would be obtained by the use of a horn—balanced rudder. The ratio would of course be affected by the size of the horn balance and the location of

the horizontal tail. A study of figure 10 indicates that when the
unshielded part of the overhang-balanced rudder became overbalanced,
positive values of $C_{h_{\alpha_s}}$ were obtained. The horn-balanced rudder

is therefore expected to have a larger positive $C_{h_{\alpha_s}}$ when shielded

than when unshielded. As the shielding of the rudder increases, the
increase in balance of the unshielded part of the rudder probably
will result in an increase in positive $C_{h_{\alpha_s}}$ and an increase in the

range of angle of attack of the surface for which $C_{h_{\alpha_s}}$ is positive.

As the shielding increases further, the unshielded part of the rudder
becomes overbalanced and C_{h_δ} will also become positive. For this

condition, obtained at high spinning angles of attack, the rudder will
float full against the spin unless sideslip angles at the tail are
very small. The combination of high spinning angles of attack and
very small sideslip angles at the tail (an improbable attitude for a
spinning airplane) will probably cause the rudder to float full with
the spin.

In general, the horn-balanced rudder appears to be the most
adaptable for obtaining desirable floating characteristics throughout
the spinning angle-of-attack range for the spinning conditions likely
to be obtained on an airplane.

If a control surface is used which has hinge-moment-coefficient
characteristics such that it has a stabilizing floating tendency
$\left(\text{positive } C_{h_{\alpha_s}}\right)$ in normal flight attitudes, as is the case for the

14.5-percent-horn-balanced rudder presented in figure 11, lateral
oscillations of constant amplitude may be obtained in a rudder system
having friction. The cause and the conditions that tend to minimize
or eliminate these undesirable oscillations are discussed in detail
in reference 13.

Application of data to specific spinning attitudes.- For the
50 spins presented in table III, the angle of attack ranged from
about 15° to 68° and the angle of outward sideslip varied from about
2° to 33°. Spin attitudes of most personal-owner-type airplanes will
probably fall within these ranges and the floating angles shown in
figures 12 to 16 and presented in table III are practicable
indications of the floating angles that may be encountered. The data,
as previously indicated, were obtained statically and these floating
angles, therefore, do not include the effects of centrifugal and
frictional forces.

For the specific spinning attitudes for which the plain-rudder data were applied (figs. 12 to 14), the floating angles ranged from approximately neutral to full with the spin. At corresponding attitudes (fig. 16), the 27.9-percent-overhang-balanced rudder floated near neutral. The data for the horn-balanced rudder were not sufficiently extensive for specific application but, as had been stated, a horn-balanced rudder would probably have floated against the spin.

Calculations were made of the rudder-pedal force required to hold the plain rudder at neutral. This study was made because of the supposition that, as a solution to the problem of control release, the plain-rudder control system might be preloaded so that it would move to neutral when released in a spin. For the tail configurations having normal and large-size vertical tails, a preloading force of approximately 75 and 145 pounds, respectively, (table III) would be required to insure movement of the rudder to neutral; however, preloading a rudder control system by these amounts is considered objectionable.

Elevator Floating Characteristics

The floating characteristics of elevators, as of rudders, depend primarily on the aerodynamic hinge-moment coefficients of the surface, but elevators are not shielded in the manner rudders are at spinning angles of attack; however, in a spin, the horizontal tail surfaces are generally stalled because of the high angles of attack, and the variations of elevator hinge-moment coefficient with α_s and δ_e are not linear. Therefore, like the case for the rudder, $C_{h_{\alpha_s}}$ and C_{h_δ} cannot be used to calculate floating angles at spinning attitudes. In general, however, a consideration of the variation of elevator hinge-moment coefficient with α_s and δ_e should lead to a qualitative understanding of elevator floating characteristics at spinning attitudes. The ensuing analysis of the floating characteristics of the various types of elevators is made on this basis.

The curves of hinge-moment coefficient plotted against elevator deflection in figure 17 for the plain, the 35-percent-overhang-balanced, and the beveled-trailing-edge elevators were negative in slope and therefore the elevators would tend to float in an up position for all spinning angles of attack. The elevators would tend to float more upward as the angle of attack increased. At angles of attack

below 35°, the 35–percent–overhang–balanced elevator would float at the highest elevator–up position, whereas the beveled–trailing–edge elevator would float the closest to neutral. At angles of attack of 35°, 40°, and 45°, for which the 35–percent–balanced elevator would float in a full–up position, the beveled–trailing–edge elevator would float progressively more upward until it attained a 15° up deflection at an angle of attack of 45°. For spins with angles of attack higher than 45° (the limit for which data were available) the favorable floating tendency of the beveled–trailing–edge elevator may disappear. A study of reference 8 indicates that, at spinning angles of attack, varying the size of the chord of the bevel would not improve the floating tendency. The results of references 6 and 7 for a 48–percent–overhang–balanced elevator and a 50–percent–overhang–balanced elevator, respectively, indicate that elevators with such very large balances will generally float full up in spins. There is an indication, based on reference 10 and on an application of reference 9 to elevators, that with a sufficiently large horn favorable floating characteristics may be obtained, provided the spin is very steep (less than 20° angle of attack). At an angle of attack of 20°, however, $C_{h_{\alpha_s}}$ becomes negative and it is indicated that horn–balanced elevators having a balance of size suitable for normal flight will float in an up position.

The influence of tab deflections on elevator floating characteristics through the entire spinning angle–of–attack range for an elevator having a 31.8–percent overhang balance is shown in figure 18. With the tab at its neutral position, the floating characteristics of this elevator were, in general, similar to those for the 35–percent–overhang–balanced elevator (fig. 17) in that the elevators both tended to float to the full–up positions. Deflection of the small tab 14° upward did not appreciably affect the floating characteristics of the elevator although it reduced the stick force required to move the elevator down from its full–up position. The larger tab deflected 14° upward, however, made the elevator float about 10° down from neutral at an angle of attack of 18°, and as the angle of attack increased the elevator floated progressively less downward and became neutral at an angle of attack of approximately 45°.

Use of tabs deflected upward will be effective in causing elevators to float downward during a spin, the floating angle at any specific spinning angle of attack depending upon the size of the tab. A manual movement of tabs during a spin, however, would not fulfill the present Civil Air Regulations.

A study based on references 5, 7, and 8 indicates that outward sideslip in the spin does not greatly affect elevator floating characteristics. At values of outward sideslip below 10°, the effect is negligible, but for larger values of outward sideslip up to 30° the effect is such as generally to cause the elevator to float more upward.

The effects, however, do not change the general comparative floating characteristics of the elevators and the beveled—trailing—edge elevator still floats closest to neutral even with large amounts of sideslip. The characteristics of beveled—trailing—edge control surfaces including the deficiencies of this type of balance in normal flight are discussed in reference 11.

CONCLUSIONS

A study was made of available rudder and elevator hinge—moment—coefficient data in order to determine the floating characteristics of various types of rudders and elevators in spinning attitudes. Some of the data were applied to specific spin attitudes obtained on a model of a typical personal—owner—type airplane that was tested. The results of the analysis for the data presented herein indicate the following conclusions with regard to obtaining spin recovery upon releasing the controls:

1. A plain rudder generally will float with the spin for all angles of attack.

2. Of the rudders investigated, the horn—balanced rudder appears to be the most adaptable for obtaining desirable floating characteristics at spinning attitudes.

3. The partial—length overhang—balanced rudder (rudder above the horizontal tail) presented herein generally will float near neutral for low angles of attack, and for high angles of attack it should float against the spin. The full—length overhang—balanced rudder (a part of the rudder extending below the horizontal tail) may float with the spin.

4. Preloading of a plain—rudder control system in order to move the plain rudder to neutral for all probable spin conditions is objectionable because of the large amount of preloading required.

5. Plain, overhang—balanced, and beveled—trailing—edge elevators generally will float in an up position in spins and should float more upward as the angle of attack increases. The beveled—trailing—edge elevator should float closest to neutral, whereas the overhang—balanced elevator should float farthest up. Indications are that horn—balanced elevators may also float in an up position.

6. Large tabs deflected upward should cause the elevators to float down in spinning attitudes.
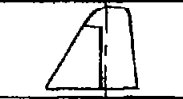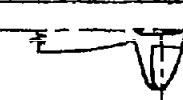

Langley Aeronautical Laboratory
    National Advisory Committee for Aeronautics
        Langley Air Force Base, Va., June 20, 1949

REFERENCES

1. Neihouse, A. I.: Tail-Design Requirements for Satisfactory Spin
   Recovery for Personal-Owner-Type Light Airplanes. NACA TN 1329,
   1947.

2. Neihouse, A. I.: A Mass-Distribution Criterion for Predicting the
   Effect of Control Manipulation on the Recovery from a Spin.
   NACA ARR, Aug. 1942.

3. Anon.: Airplane Airworthiness — Normal, Utility, Acrobatic, and
   Restricted Purpose Categories. Pt. 03 of Civil Air Regulations,
   Civil Aero. Board, U.S. Dept. Commerce, Dec. 15, 1946, pp. 11–12,
   secs. 03.135-N — 03.135-A.

4. Stone, Ralph W., Jr., and Burk, Sanger M., Jr.: Effect of
   Horizontal-Tail Position on the Hinge Moments of an Unbalanced
   Rudder in Attitudes Simulating Spin Conditions. NACA TN 1337,
   1947.

5. Stone, Ralph W., Jr., and Burk, Sanger M., Jr.: Hinge-Moment
   Characteristics of Balanced Elevator and Rudder for a Specific
   Tail Configuration on a Fuselage in Spinning Attitudes. NACA
   TN 1400, 1947.

6. Hoggard, H. Page, Jr., and Hagerman, John R.: Tests of 0.14-Scale
   Models of the Control Surfaces of Army Project MX-511 in
   Attitudes Simulating Spins. NACA MR L5D12a, 1945.

7. Sears, Richard I., and Hoggard, H. Page, Jr.: Characteristics of
   Plain and Balanced Elevators on a Typical Pursuit Fuselage at
   Attitudes Simulating Normal-Flight and Spin Conditions. NACA
   ARR, March 1942.

8. Gillis, Clarence L.: Characteristics of Beveled-Trailing-Edge
   Elevators on a Typical Pursuit Fuselage at Attitudes Simulating
   Normal Flight and Spin Conditions. NACA ARR, Dec. 1942.

9. Lowry, John G., Maloney, James A., and Garner, I. Elizabeth: Wind-
   Tunnel Investigation of Shielded Horn Balances and Tabs on a
   0.7-Scale Model of XF6F Vertical Tail Surface. NACA ACR 4C11,
   1944.

10. Lowry, John G., and Crandall, Stewart M.: Wind-Tunnel Investigation
    of Unshielded Horn Balances on a Horizontal Tail Surface. NACA
    TN 1377, 1947.

11. Sears, Richard I.: Wind-Tunnel Data on the Aerodynamic Charac-
    teristics of Airplane Control Surfaces. NACA ACR 3L08, 1943.

12. Zimmerman, C. H.: Preliminary Tests in the N.A.C.A. Free-
    Spinning Wind Tunnel. NACA Rep. 557, 1936.

13. Greenberg, Harry, and Sternfield, Leonard: A Theoretical
    Investigation of the Lateral Oscillations of an Airplane with
    Free Rudder with Special Reference to the Effect of Friction.
    NACA Rep. 762, 1943.

TABLE I.— RANGE OF ANGLES OF ATTACK AND SIDESLIP AND OF CONTROL DEFLECTIONS FOR

THE CONTROL-SURFACE HINGE-MOMENT-COEFFICIENT DATA OBTAINED FROM REFERENCES

Control surface		Reference	δ_r (deg)	δ_e (deg)	α (deg)	β_t (deg)
	Plain rudder	4	30 to −30	0	10 to 70	0 to −30
	Balanced rudder with a 27.9-percent-area overhang	5	25 to −25	20 to −30	18 to 68	0 to −20
	Balanced rudder with a 14.5-percent-area horn	9	32 to −32	(a)	0	0 to −30
	Plain elevator and balanced elevator with a 35-percent-chord overhang	7	(a)	5 to −30	15 to 45	0
	$0.10c_e$ beveled-trailing-edge elevator	8	(a)	5 to −30	15 to 45	0
	Balanced elevator with a 31.8-percent-area overhang with and without tabs deflected −14°	5	0	20 to −30	18 to 68	0

[a]Hinge-moment coefficients obtained for a control surface not in the presence of a tail assembly.

NACA

TABLE II.— DIMENSIONAL, MASS, AND INERTIA CHARACTERISTICS

OF THE REPRESENTATIVE PERSONAL—OWNER—TYPE AIRPLANE

[Full—scale values given; moment—of—inertia values
are about the center of gravity]

Length, average over—all, ft 22.40

Wing:
    Span, ft 33.82
    Area, sq ft 163.4
    Section . . . . NACA 23012
    Twist, deg 0
    Incidence, deg 3
    Dihedral, deg 6
    Mean aerodynamic chord, c', in. 58.65
    Distance of leading edge of mean aerodynamic chord
       rearward of leading edge of wing, in. 0.62

Ailerons:
    Area rearward of hinge line, sq ft 15.70
    Chord, rearward of hinge line, ft 1.09
    Span, percent of wing span 42.5

Horizontal tail surfaces (normal size):
    Total area, sq ft 26.27
    Tail span, ft 10.25
    Dihedral of tail, deg 0
    Distance from normal center of gravity to
       elevator hinge line, ft 13.72
    Section . . . . Modified NACA 0009

Horizontal tail surfaces (large size):
    Total area, sq ft 37.58
    Tail span, ft 12.25
    Dihedral of tail, deg 0
    Distance from normal center of gravity to
       elevator hinge line, ft 13.72
    Section . . . . Modified NACA 0009

~NACA~

TABLE II.- DIMENSIONAL, MASS, AND INERTIA CHARACTERISTICS

OF THE REPRESENTATIVE PERSONAL-OWNER-TYPE AIRPLANE — Continued

Vertical tail surfaces (normal size):
    Offset, deg   0
    Total area, sq ft 12.96
    Total unbalanced rudder area, rearward of
        hinge line, sq ft 6.48
    Rudder root-mean-square chord, ft 1.30
    Rudder height along hinge line, ft 5.32
    Distance from normal center of gravity to rudder
        hinge line, ft 14.17
    Section . . . . Modified NACA 0009

Vertical tail surfaces (large size):
    Offset, deg   0
    Total area, sq ft 24.56
    Total unbalanced rudder area, rearward of
        hinge line, sq ft 12.28
    Rudder root-mean-square chord, ft 1.59
    Rudder height along hinge line, ft 8.20
    Distance from normal center of gravity to rudder
        hinge line, ft 14.17
    Section . . . . Modified NACA 0009

Weight, lb 2185

Normal center-of-gravity location:
    x/c' 0.250
    z/c' 0.093

Airplane relative density, at 5000 ft, μ 6.00

Moments of inertia:
    I_X, slug-ft^2 1080

    I_Y, slug-ft^2 2012

    I_Z, slug-ft^2 3041

TABLE II.— DIMENSIONAL, MASS, AND INERTIA CHARACTERISTICS

OF THE REPRESENTATIVE PERSONAL—OWNER—TYPE AIRPLANE — Concluded

Inertia parameters:

$$\frac{I_X - I_Y}{mb^2} \quad \ldots \ldots \ldots \ldots \ldots \ldots \ldots \ldots \quad -120 \times 10^{-4}$$

$$\frac{I_Y - I_Z}{mb^2} \quad \ldots \ldots \ldots \ldots \ldots \ldots \ldots \ldots \quad -133 \times 10^{-4}$$

$$\frac{I_Z - I_X}{mb^2} \quad \ldots \ldots \ldots \ldots \ldots \ldots \ldots \ldots \quad 253 \times 10^{-4}$$

TABLE III.— FREE–SPINNING CHARACTERISTICS OF A TYPICAL PERSONAL–OWNER–TYPE

AIRPLANE AND ITS RUDDER FLOATING CHARACTERISTICS

[Model values converted to corresponding full–scale values;
right spins; δr = -30°]

| Figure	Tail	Test	Control setting		Spinning conditions					Plain rudder			Overhang-balanced-rudder floating angle (deg)
			Ailerons	Elevator	R_S (ft)	Ω (radians/sec)	V (ft/sec)	α (deg)	β_t (deg)	Floating angle (deg)	$(c_h)_{\delta_r=0°}$	F (lb)	
7(a)	1	1	20° with	20° down	4.60	4.96	170.4	15.9	-13.2	-11.5	-0.10	67.2	0
		2	Neutral	30° up	12.80	2.13	141.5	29.0	-13.7	-14.5	-.07	32.4	0
		3	20° against	30° up	13.02	2.09	130.6	29.5	-21.9	-24.5	-.14	55.2	-5.0
		4	Neutral	20° down	5.90	2.99	123.2	31.2	-21.4	-24.5	-.13	45.3	-2.5
		5	20° against	20° down	5.94	2.74	93.6	54.1	-30.2	-28.5	-.14	28.4	---
	2	6	7° with	30° up	13.35	1.98	136.2	31.6	-11.3	-6.0	-.03	12.9	-1.5
		7	20° with	30° up	9.93	1.99	120.7	39.3	-3.4	-3.5	-.02	6.7	0
	3	8	Neutral	20° down	6.30	3.30	146.1	25.1	-20.0	-22.5	-.14	69.1	---
		9	7° with	30° up	11.97	1.95	126.0	35.3	-12.4	-7.0	-.05	18.4	---
		10	20° against	20° down	6.50	2.59	115.8	36.5	-22.1	-16.5	-.11	34.1	---
		11	20° with	30° up	7.90	2.09	110.5	42.9	-9.6	-1.5	-.01	2.8	---
7(b)	4	12	Neutral	30° up	12.17	2.35	138.7	25.6	-12.7	-12.5	-.07	31.1	0
		13	20° against	30° up	14.01	2.05	141.5	28.7	-13.0	-12.5	-.05	23.2	1.0
		14	7° against	20° up	8.03	2.62	141.5	30.3	-19.9	-23.0	-.11	51.0	---
		15	Neutral	Neutral	1.95	3.10	128.5	32.3	-18.2	-20.0	-.10	38.2	0
		16	Neutral	15° down	3.82	3.18	118.3	39.8	-23.4	-22.0	-.09	29.1	---
		17	Neutral	15° down	3.62	2.86	96.1	47.4	-24.0	-12.0	-.04	8.5	---
		18	Neutral	20° down	3.13	2.89	93.6	50.9	-26.3	-17.0	-.07	14.2	---
		19	20° against	20° down	1.87	3.10	89.1	60.8	-27.6	-30.0	-.14	25.7	---
		20	20° against	Neutral	1.75	3.12	89.1	62.1	-30.4	-30.0	-.20	36.8	---
		21	Neutral	Neutral	.94	3.98	81.7	65.1	-32.7	-30.0	-.28	43.2	---
		22	Neutral	20° down	1.16	3.38	79.2	67.6	-32.8	-30.0	-.29	42.1	---
	5	23	20° with	Neutral	4.60	4.55	199.9	18.7	-9.2	-7.5	-.08	73.9	0
		24	Neutral	30° up	10.86	2.34	146.1	28.4	-14.4	-16.5	-.07	34.6	---
		25	7° with	30° up	10.91	2.29	146.1	29.4	-10.9	-6.0	-.03	14.8	---
		26	20° against	30° up	7.25	2.59	126.0	33.5	-21.3	-22.0	-.12	44.1	---
		27	Neutral	Neutral	5.22	2.93	120.7	35.7	-21.2	-20.0	-.10	33.7	---
		28	Neutral	20° down	4.20	2.95	108.4	41.4	-23.6	-20.0	-.10	27.1	---
		29	20° against	Neutral	3.12	2.75	93.6	53.8	-28.3	-27.0	-.12	24.3	---
		30	20° against	20° down	2.65	2.86	96.1	56.1	-28.5	-27.0	-.13	27.8	---
	6	31	Neutral	30° up	14.47	2.06	146.1	27.7	-12.2	-10.0	-.05	24.7	---
		32	7° against	20° up	10.27	2.43	146.1	28.1	-16.7	-17.0	-.18	49.4	---
		33	7° with	30° up	13.29	2.09	141.5	29.0	-10.0	-5.5	-.03	13.9	---
		34	7° with	20° up	9.79	2.41	148.5	29.5	-13.2	-10.0	-.06	30.6	---
		35	20° with	20° up	7.84	2.64	144.0	30.5	-2.2	-10.0	-.01	4.8	---
		36	Neutral	20° down	4.81	3.35	120.7	30.8	-25.0	-30.0	-.17	57.3	---
		37	20° against	30° up	10.66	2.23	141.5	31.3	-2.5	-10.0	-.01	4.6	---
		38	20° against	20° down	5.22	2.99	108.4	34.6	-26.6	-27.0	-.17	46.2	---
7(c)	7	39	20° with	20° down	5.04	4.06	151.0	21.2	-10.1	-7.5	-.07	86.2	-3.5
		40	Neutral	20° down	5.15	3.43	136.2	28.0	-19.8	-23.0	-.12	120.2	---
		41	7° with	30° up	11.62	1.92	118.3	36.9	-14.7	-13.5	-.03	22.7	---
		42	20° with	30° up	9.33	2.14	128.5	37.0	-1.7	-2.5	-.01	8.9	5.0
		43	20° against	20° down	3.47	2.56	93.6	54.8	-26.9	-24.5	-.08	37.9	---
		44	Neutral	20° down	2.84	2.56	91.2	60.0	-23.0	-19.0	-.03	13.5	---
	8	45	Neutral	20° down	5.70	3.28	133.8	27.7	-22.1	-24.0	-.15	145.0	---
		46	7° against	20° up	9.08	2.45	141.5	30.6	-17.7	-15.0	-.09	97.3	---
		47	Neutral	20° up	10.81	2.11	141.5	33.8	-14.9	-12.5	-.06	64.9	---
		48	7° with	30° up	10.17	2.07	128.5	36.5	-15.3	-10.5	-.06	53.5	1.5
		49	20° with	30° up	8.04	2.03	110.5	44.2	-9.4	1.5	.01	-6.6	-5.0
		50	20° against	20° down	3.18	2.58	96.1	56.7	-26.1	-25.5	-.11	54.8	---

NACA
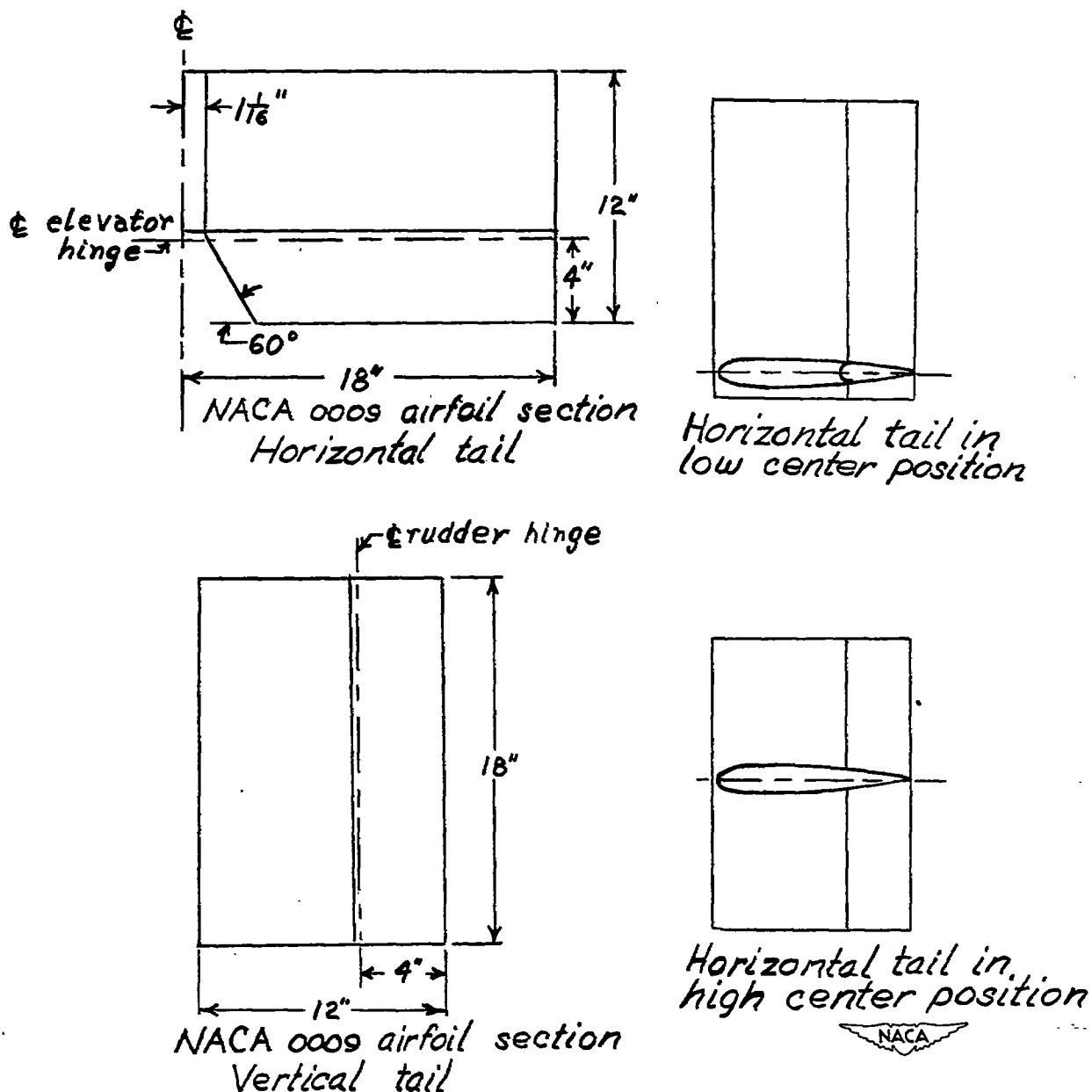
Figure 1.— Details of horizontal and vertical tails and sketch of tail
configurations previously tested (reference 4) to obtain rudder
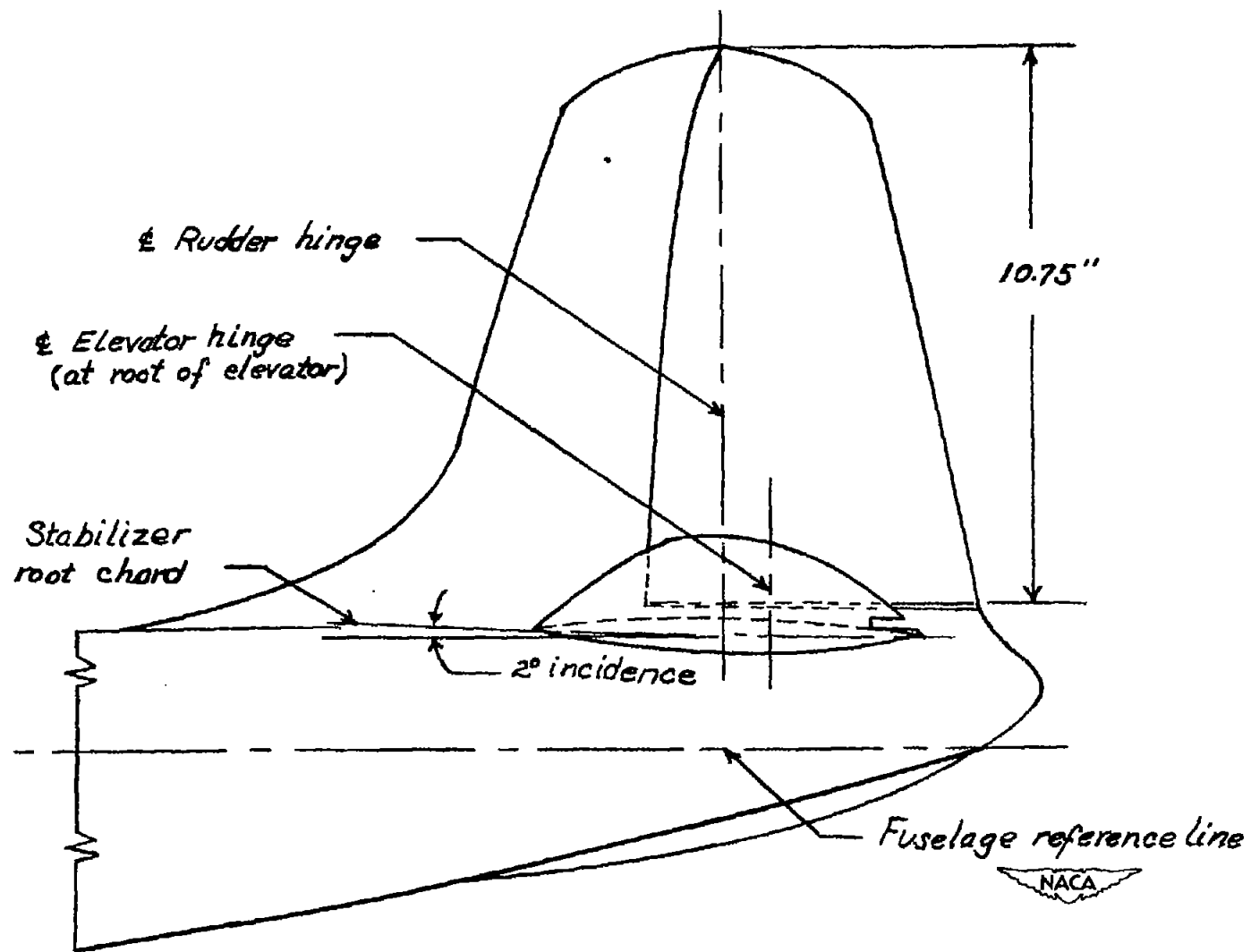hinge—moment—coefficient data for a plain rudder.

Figure 2.— Drawing of tail assembly previously tested (reference 5) to obtain rudder hinge-moment-coefficient data for a 27.9-percent-overhang-balanced rudder.
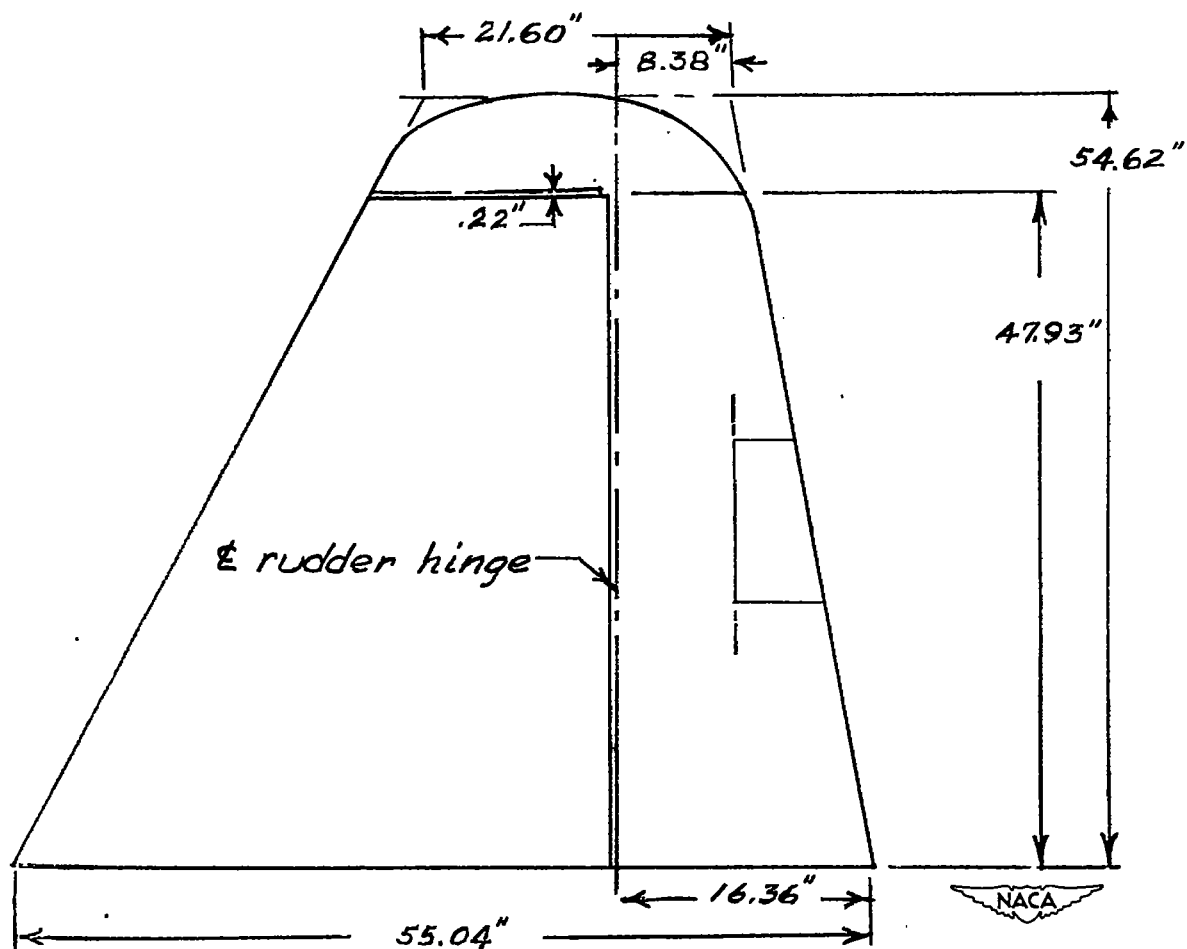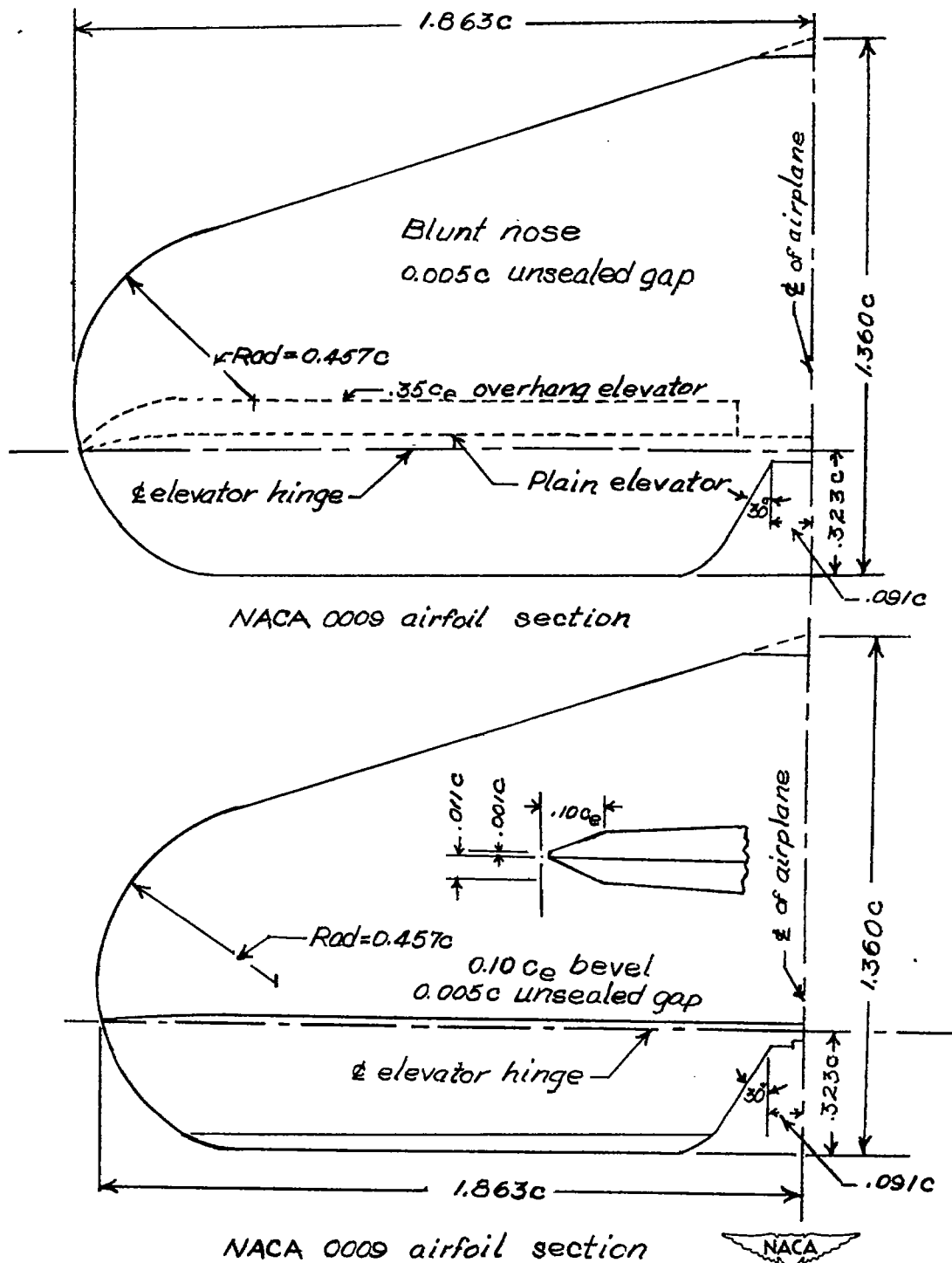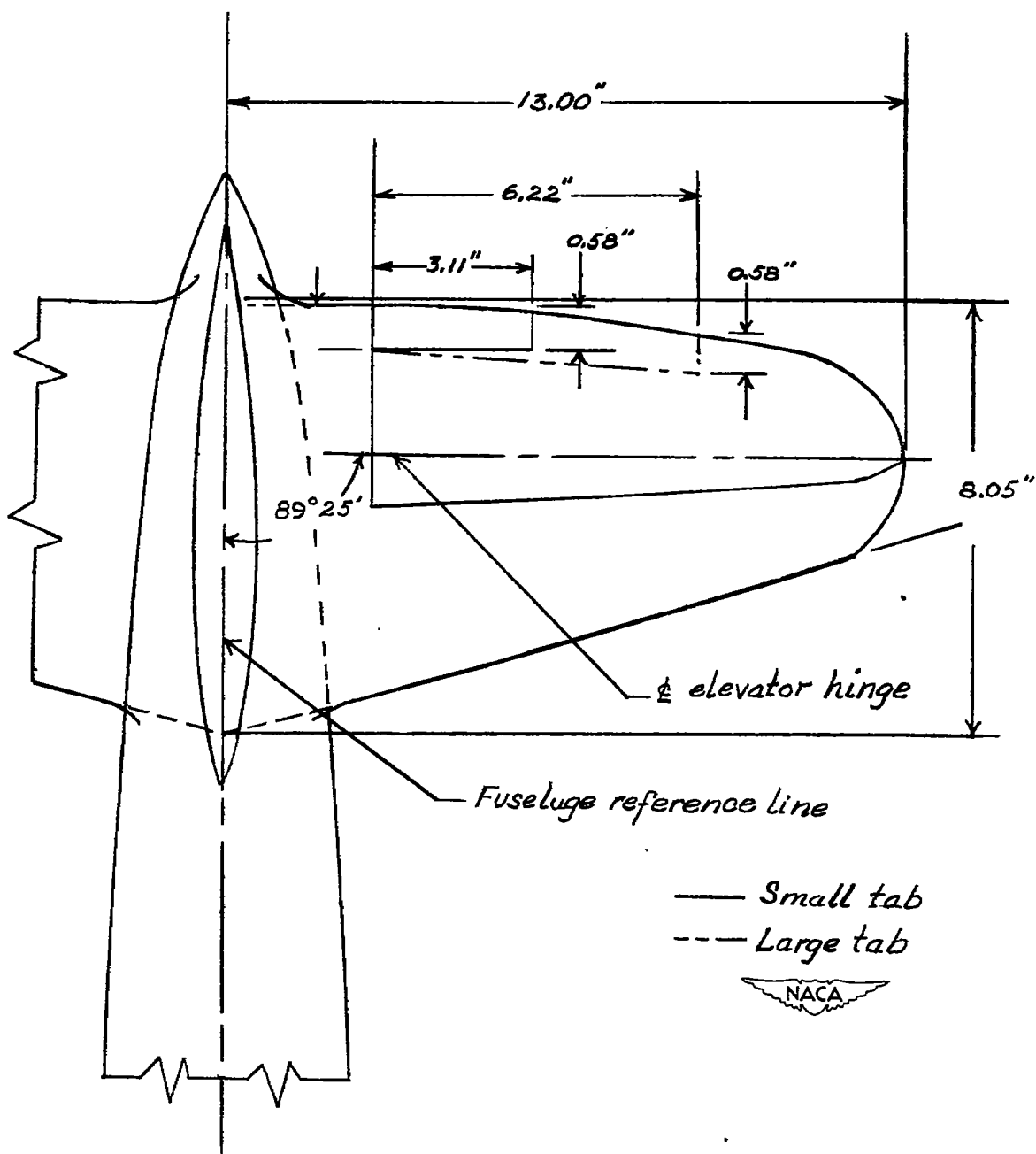
Figure 3.— Plan view of vertical tail previously tested (reference 9) to obtain rudder hinge-moment-coefficient data for a 14.5-percent-horn-balanced rudder.

Figure 4.— Details of horizontal tails previously tested to obtain elevator hinge-moment-coefficient data for a plain and a 35-percent-overhang-balanced elevator (reference 7) and a 0.10c_e beveled-trailing-edge elevator (reference 8).

13.00"

6.22"

3.11"

0.58"

0.58"

89°25'

8.05"

₵ elevator hinge

Fuseluge reference line

——— Small tab

– – – Large tab

NACA

Figure 5.— Details of a horizontal tail previously tested (reference 5)
to obtain elevator hinge—moment—coefficient data for a 31.8—percent—
overhang—balanced elevator with tabs.
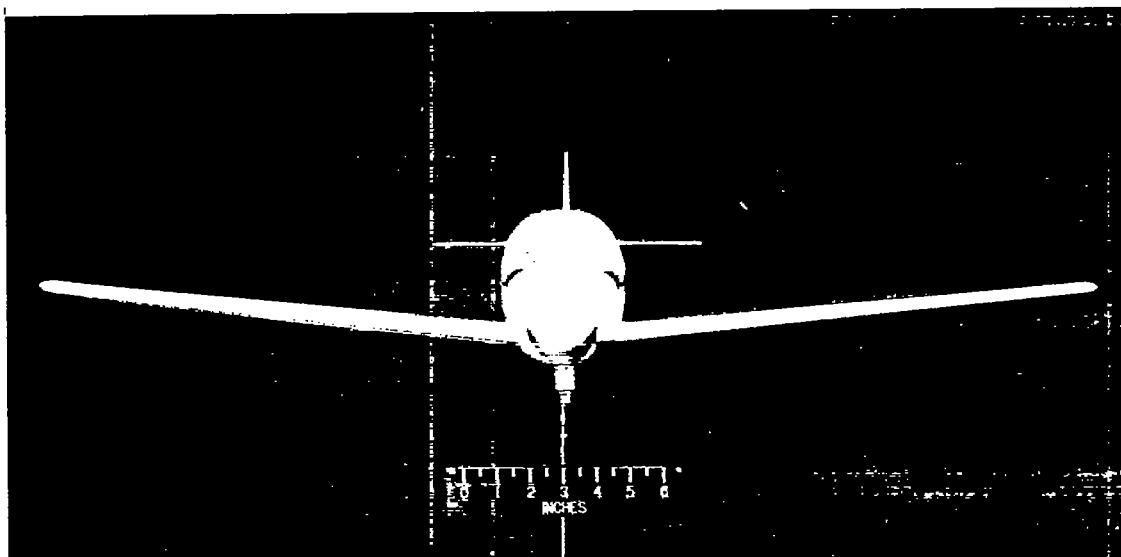
(a) Front view.
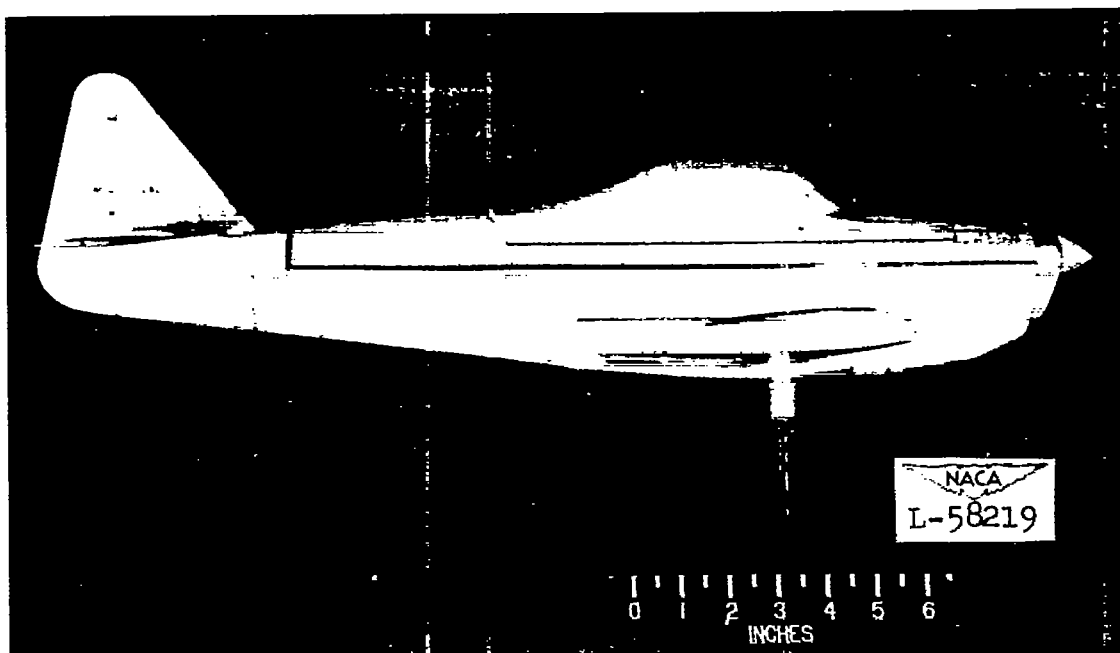
(b) Side view.

Figure 6.— Photographs of the $\frac{1}{12.4}$—scale model of the typical personal—owner—type airplane tested in the Langley 20—foot free—spinning tunnel.
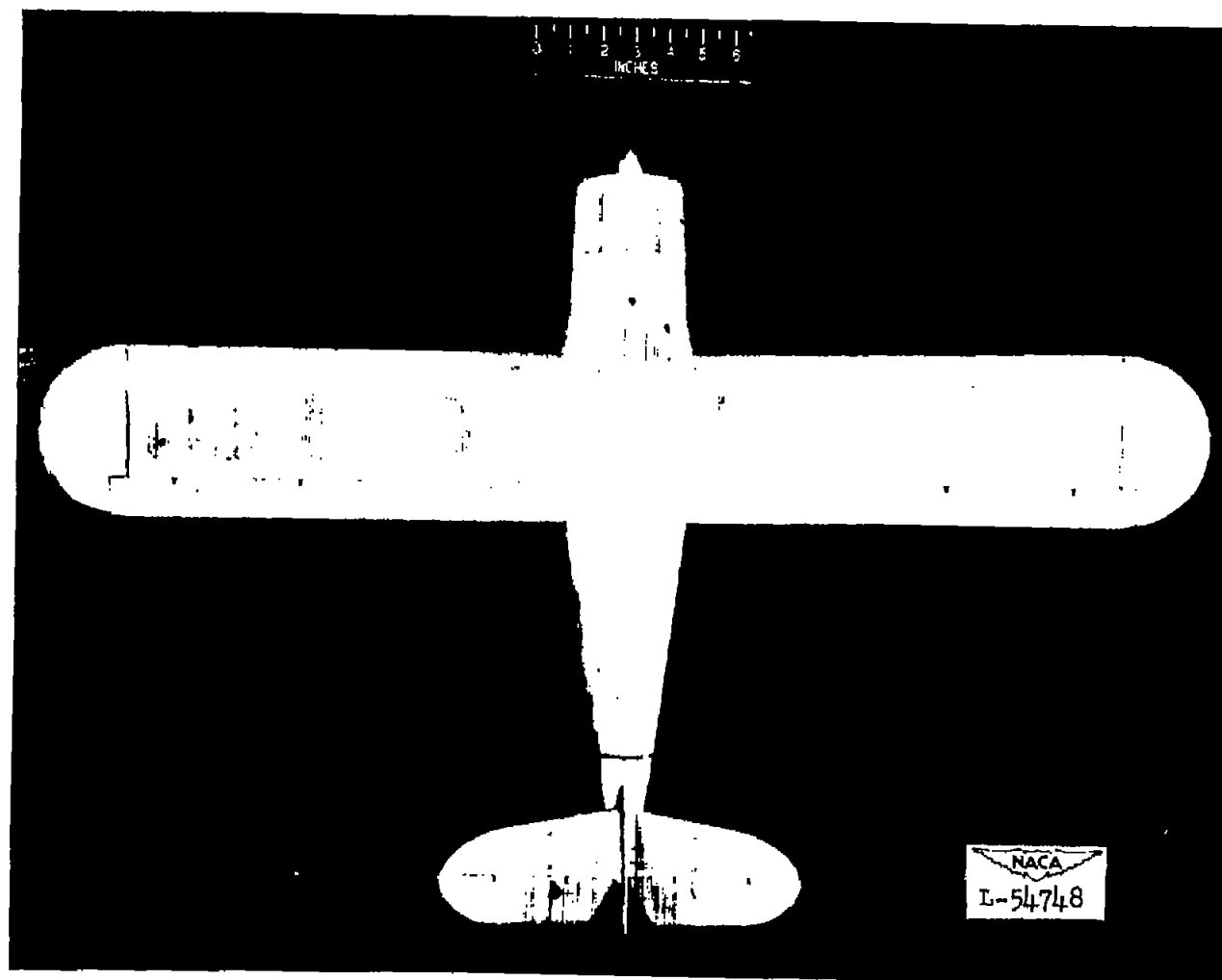
(c) Plan view.

Figure 6.— Concluded.

	Horizontal tail size	Vertical tail size	Y (ft)
Tail 1	Normal	Normal	0.23
Tail 2	Normal	Normal	-.67
Tail 3	Normal	Normal	-1.93

1.07'

4.24'

Tail 3

Tail 2

Tail 1

₵ rudder hinge

Fuselage reference line

Y

₵ elevator hinge

NACA

3.32'
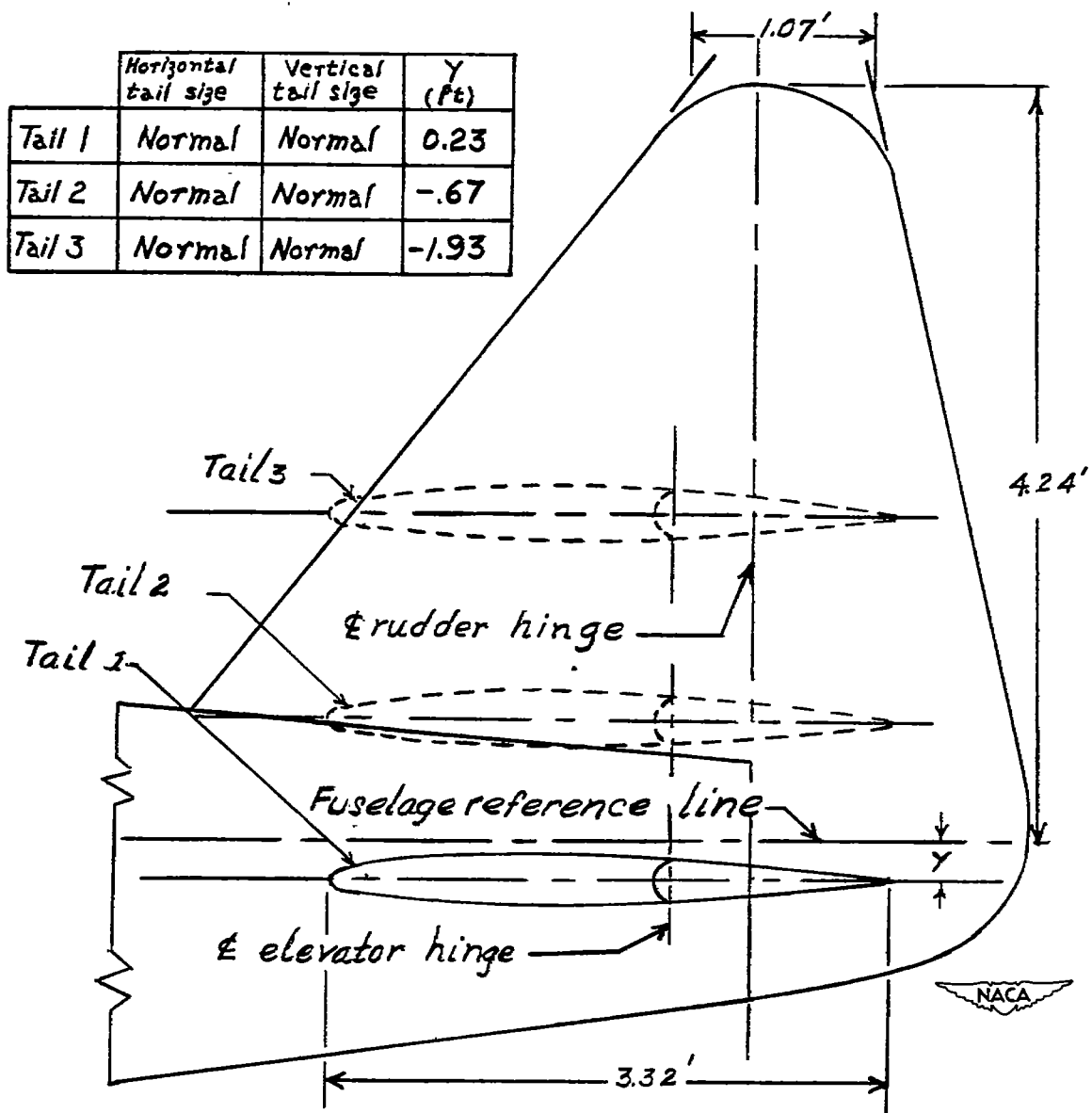
(a) Tails 1, 2, and 3.

Figure 7.— Tail configurations tested on the typical personal—owner—type airplane. All dimensions are full scale.

	Horizontal tail size	Vertical tail size	Y (Ft)
Tail 4	Large	Normal	0.21
Tail 5	Large	Normal	-.52
Tail 6	Large	Normal	-1.70

1.07'

4.24'

Tail 6

Tail 5

Tail 4

₵ rudder hinge

Fuselage reference line

Y

₵ elevator hinge

NACA

4.13'
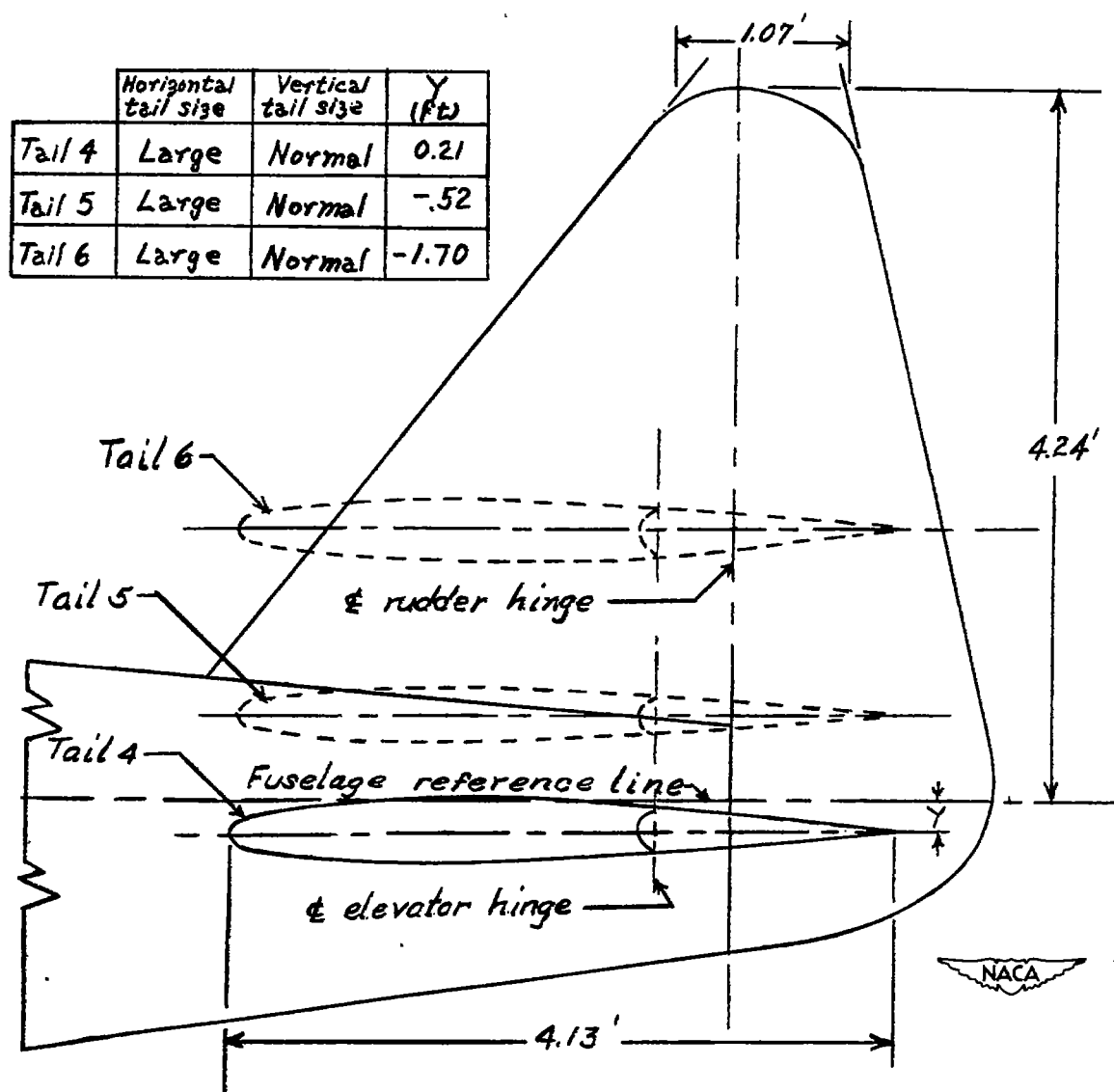
(b) Tails 4, 5, and 6.

Figure 7.— Continued.

	Horizontal tail size	Vertical tail size	Y (ft)
Tail 7	Normal	Large	0.67
Tail 8	Normal	Large	-1.25

1.34'

7.12'

Tail 8

Tail 7

₡ rudder hinge

₡ elevator hinge

Y

Fuselage reference line

3.32'
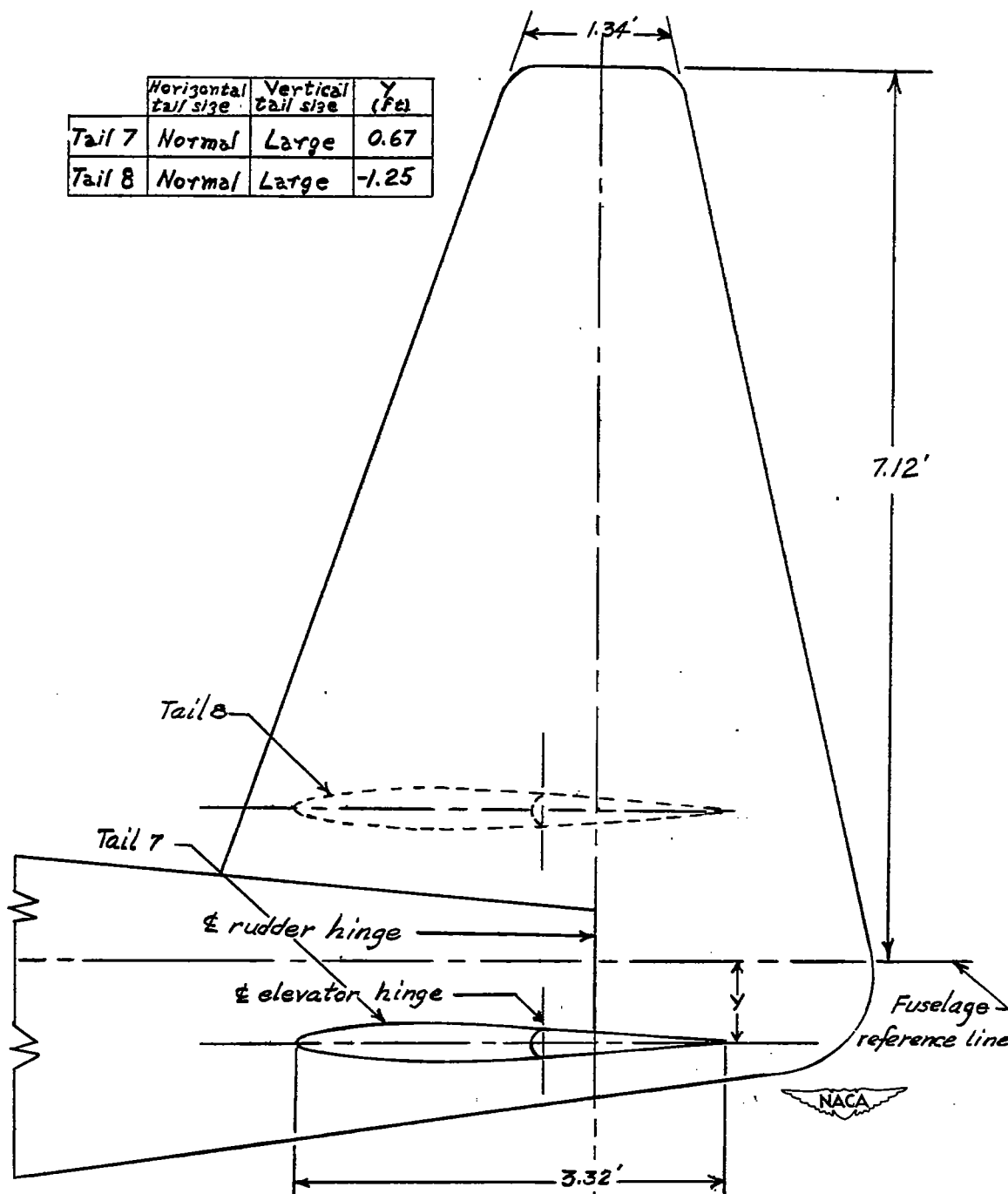
(c) Tails 7 and 8.

Figure 7.— Concluded.
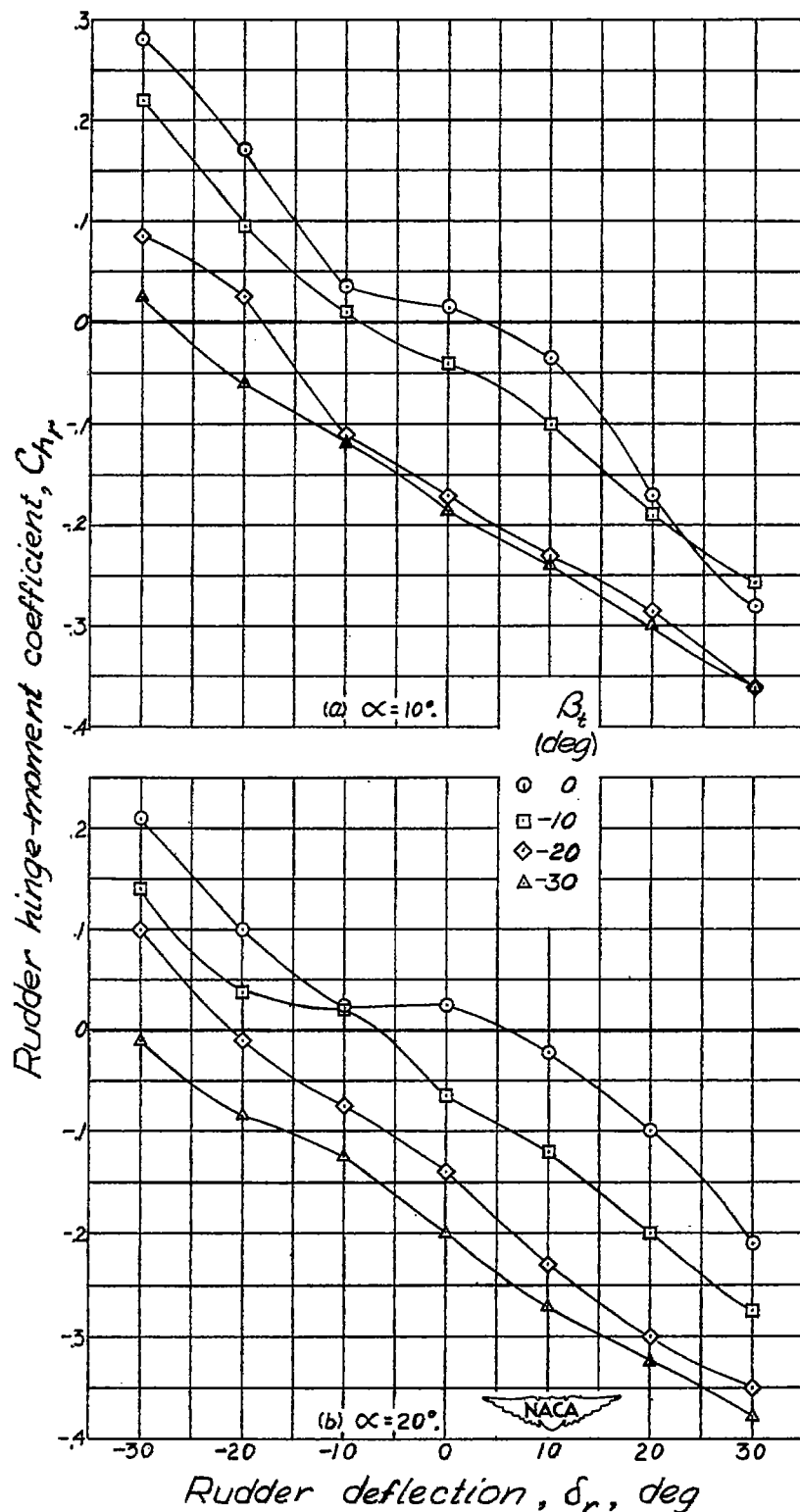
Figure 8.— Rudder hinge-moment coefficient as a function of rudder
    deflection for various angles of sideslip at specific angles of
    attack. Plain rudder; horizontal tail in low position; $\delta_e = 0^\circ$.
Data from reference 4.
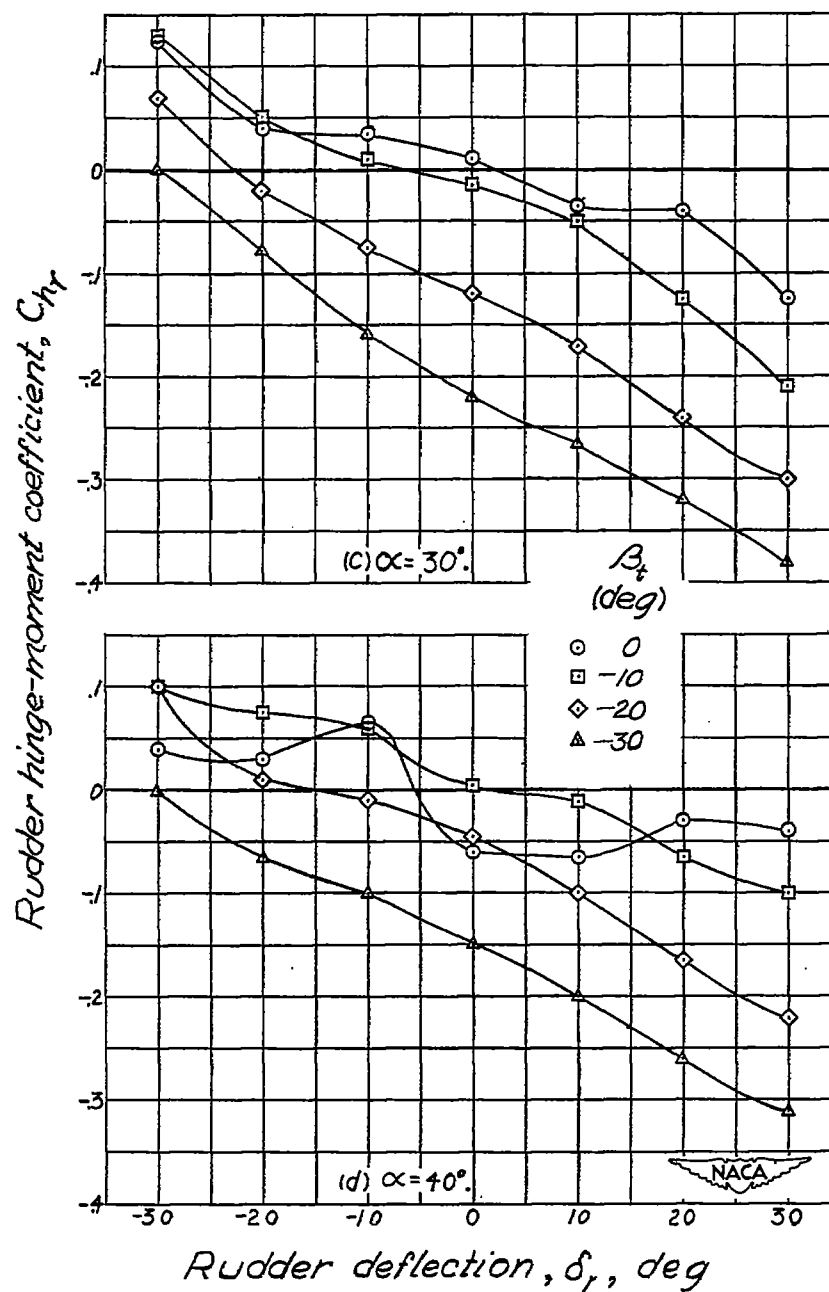
Figure 8.— Continued.
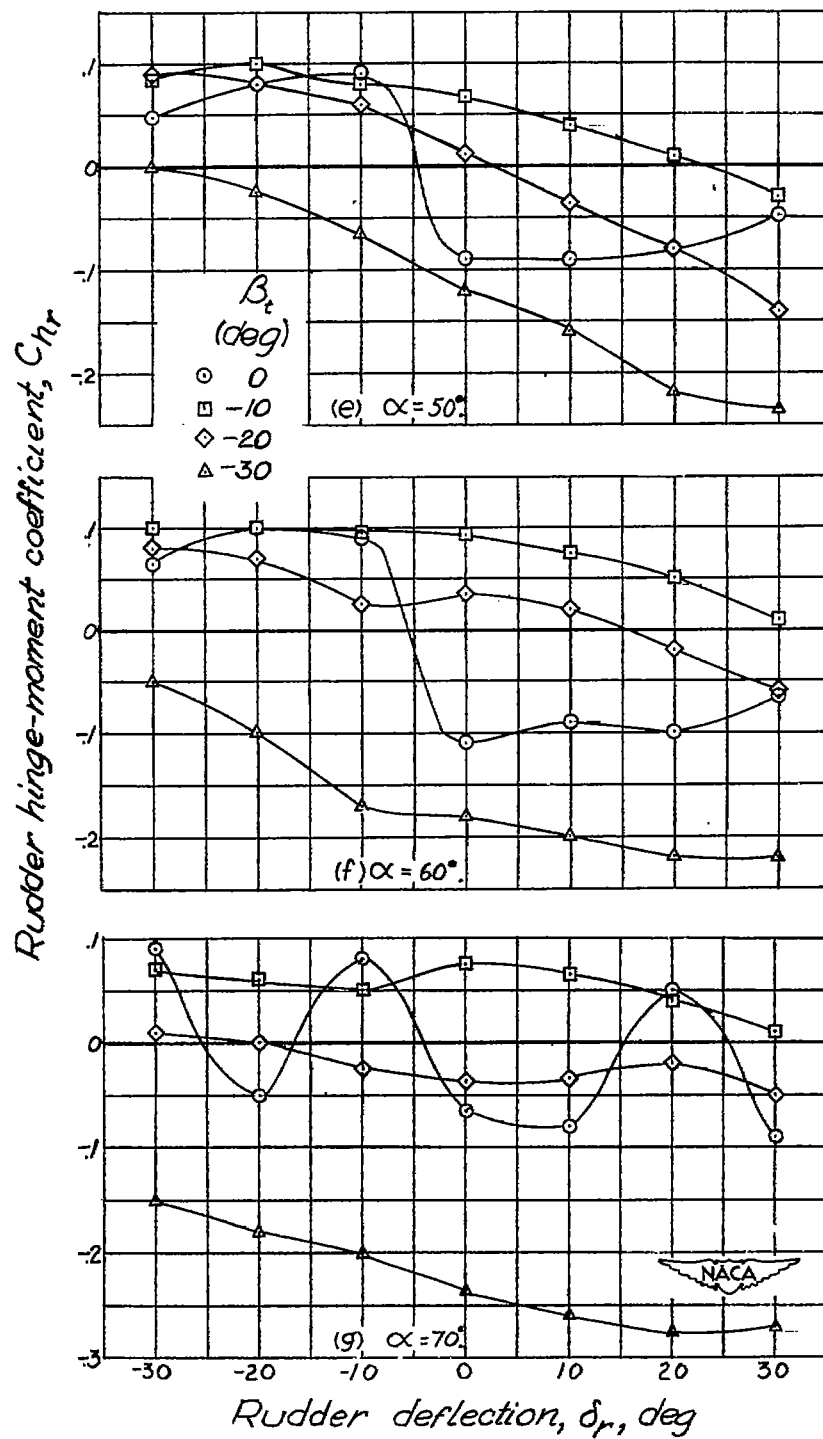
Figure 8.— Concluded.
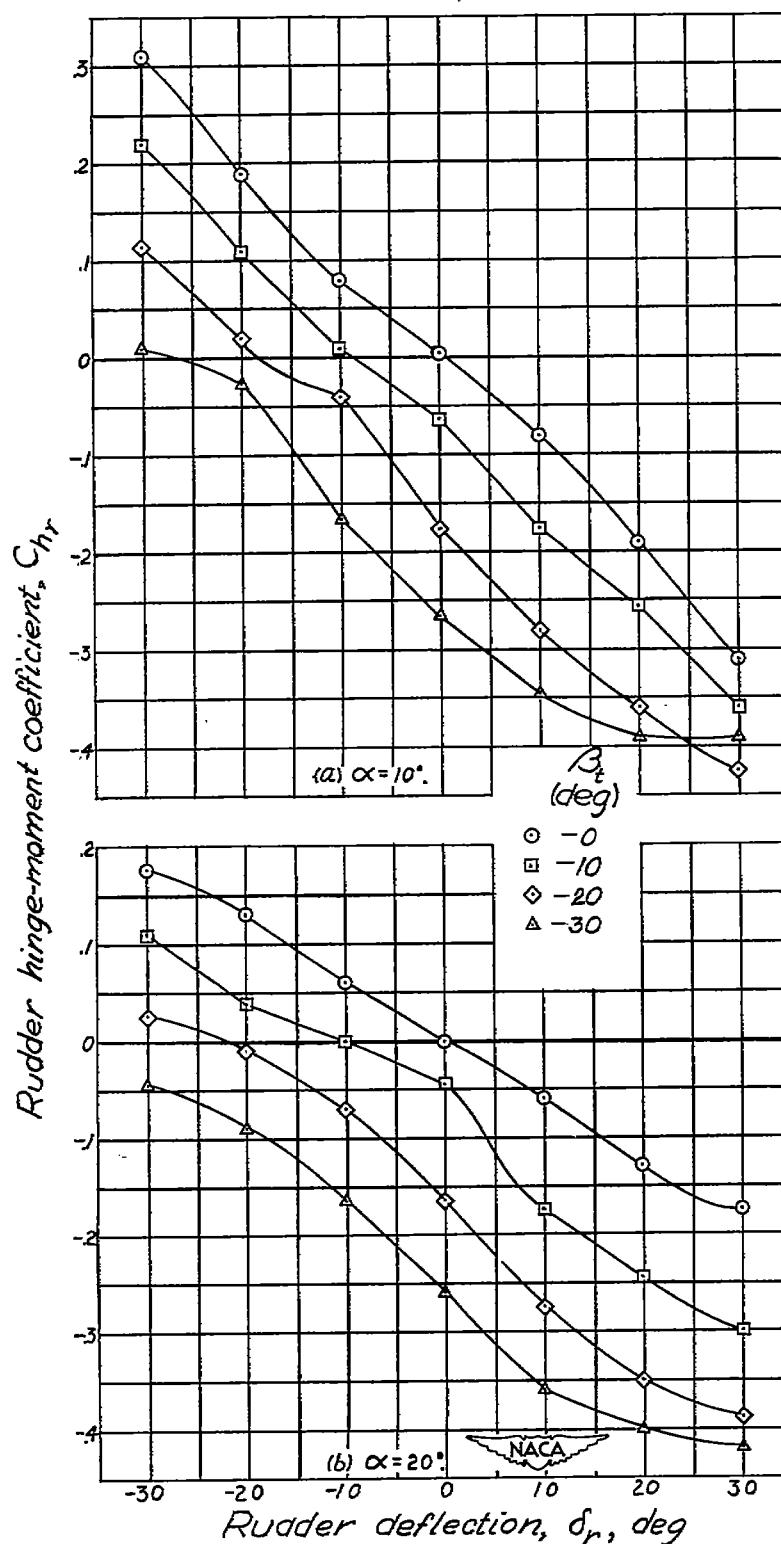
Figure 9.— Rudder hinge–moment coefficient as a function of rudder
   deflection for various angles of sideslip at specific angles of
   attack. Plain rudder; horizontal tail in high position; $\delta_e = 0^\circ$.
Data from reference 4.
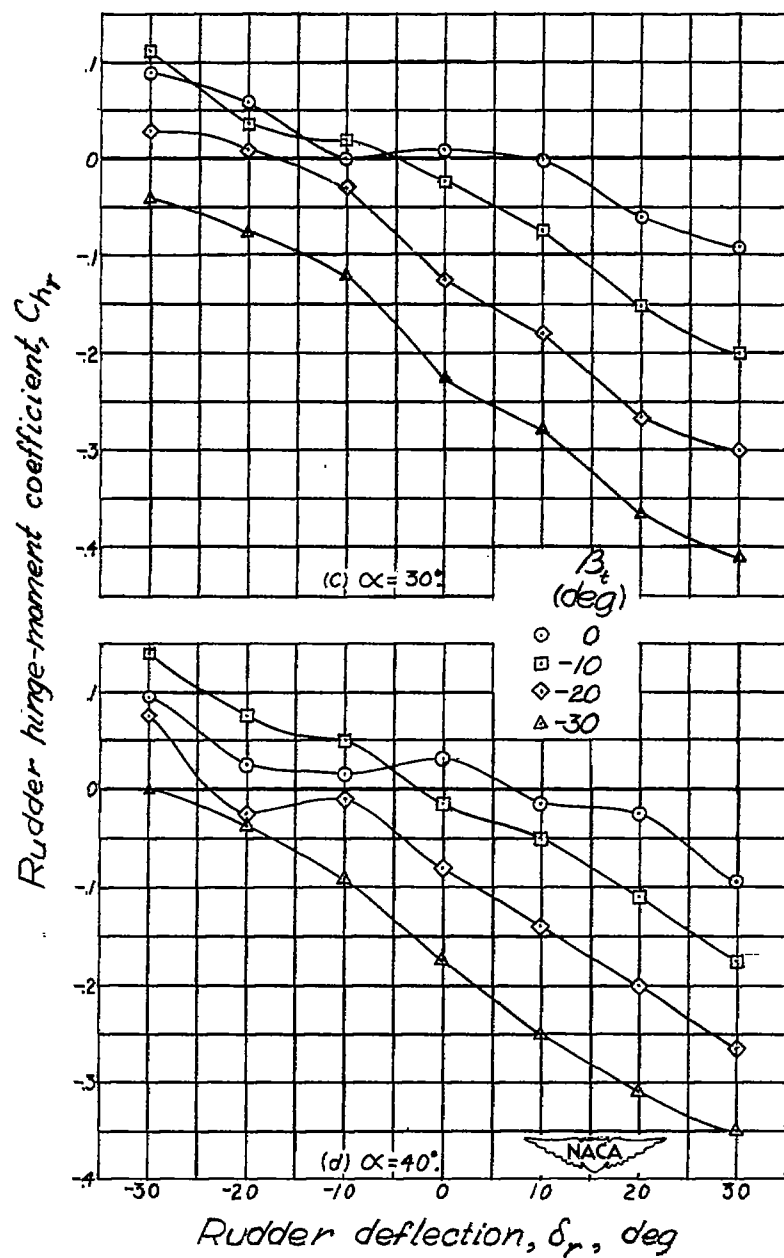
Figure 9.— Continued.
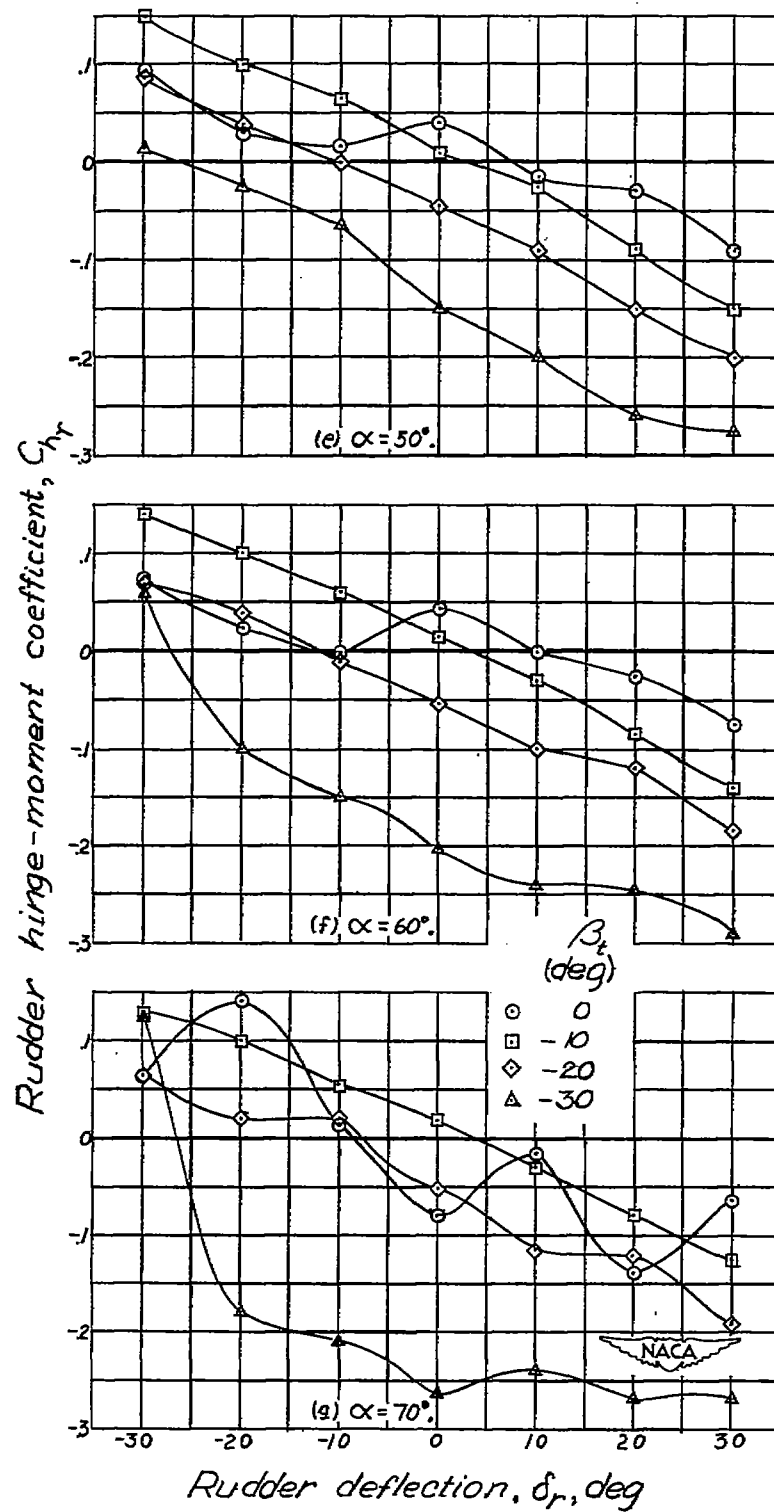
Figure 9.— Concluded.
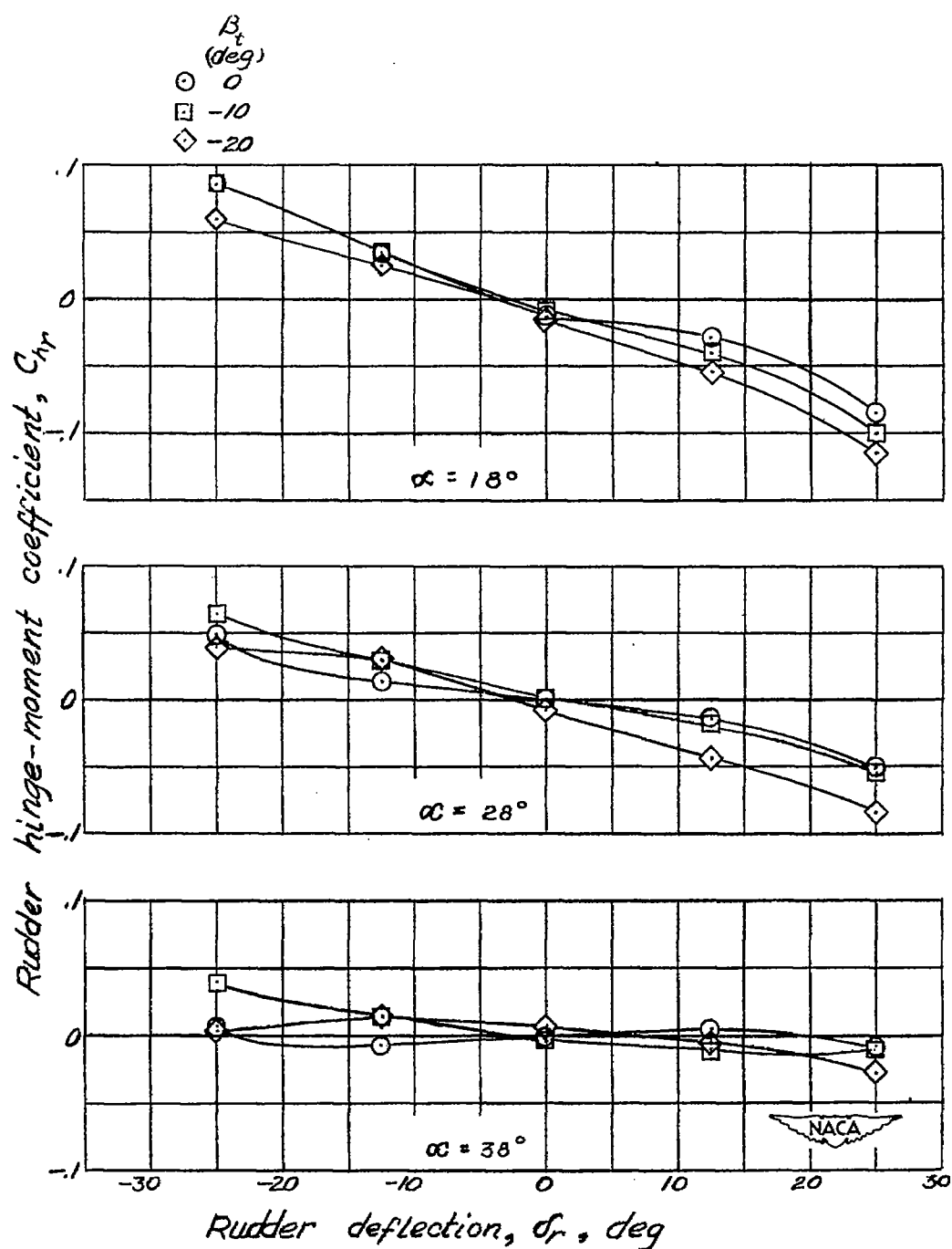
(a) $\delta_e = -30°$.

Figure 10.— Rudder hinge-moment coefficient as a function of rudder
deflection for various angles of sideslip at specific angles of
attack. 27.9-percent-overhang-balanced rudder. Data from
reference 5.
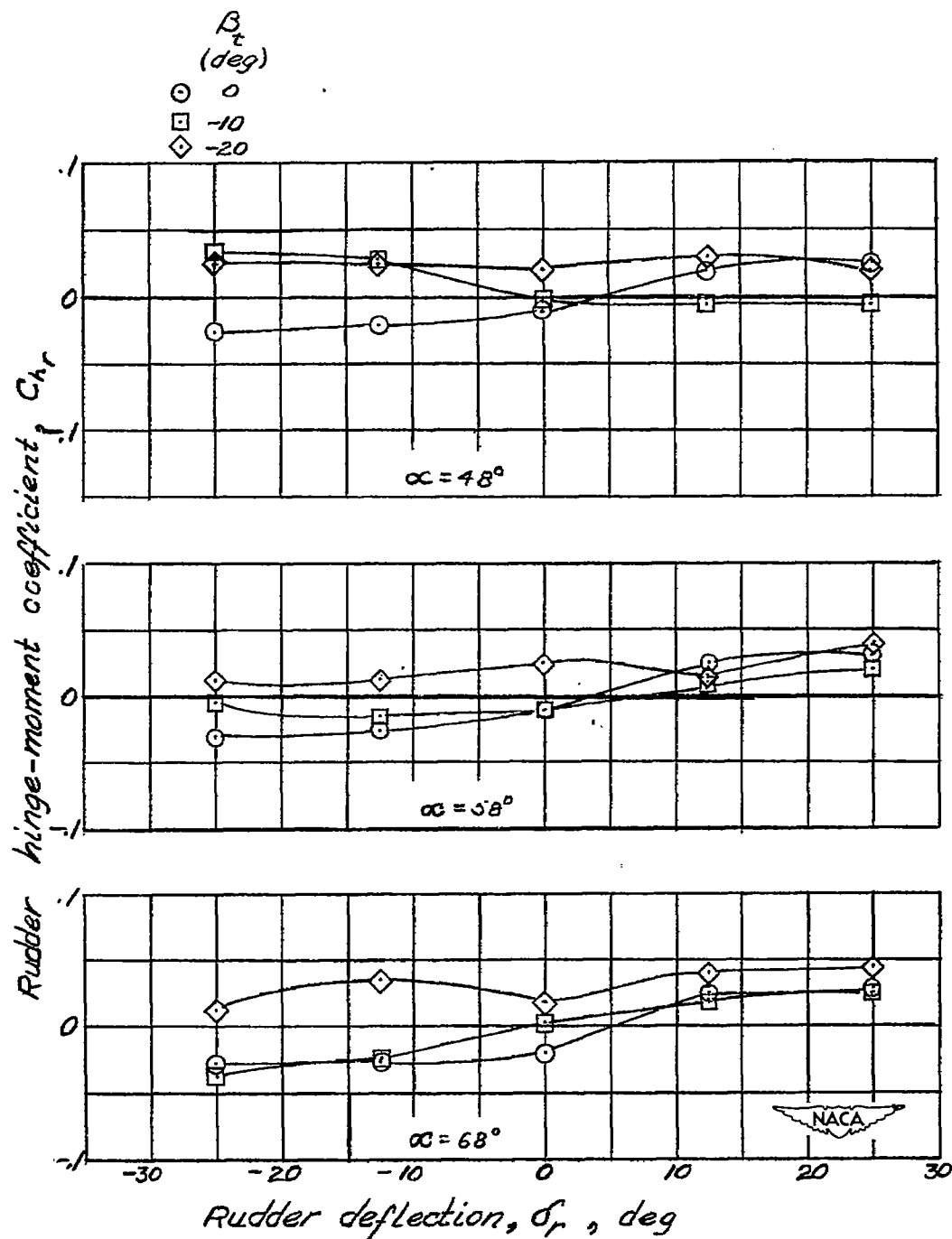
(a) Concluded. $\delta_e = -30^\circ$.

Figure 10.— Continued.
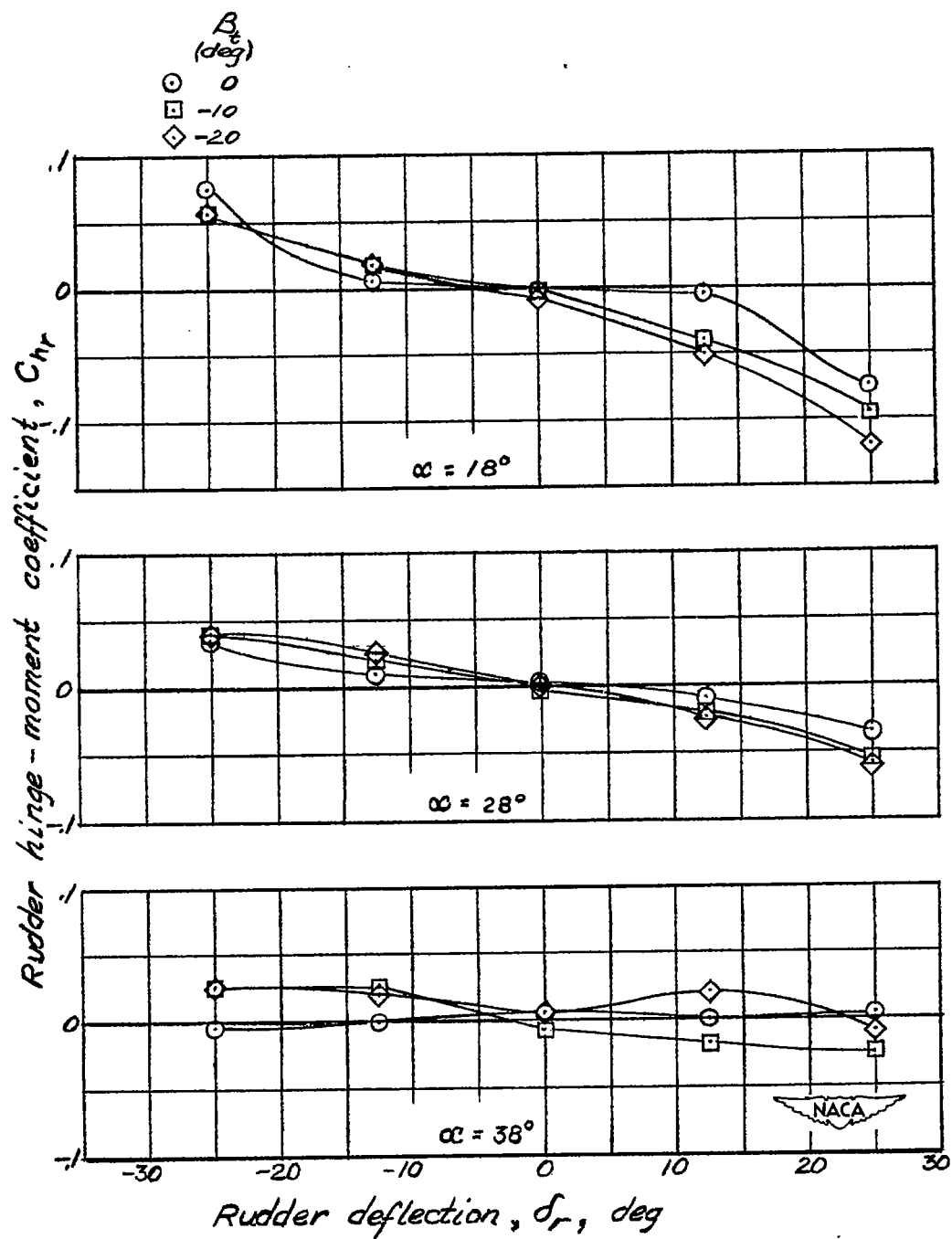
(b) $\delta_e = 0°$.

Figure 10.— Continued.
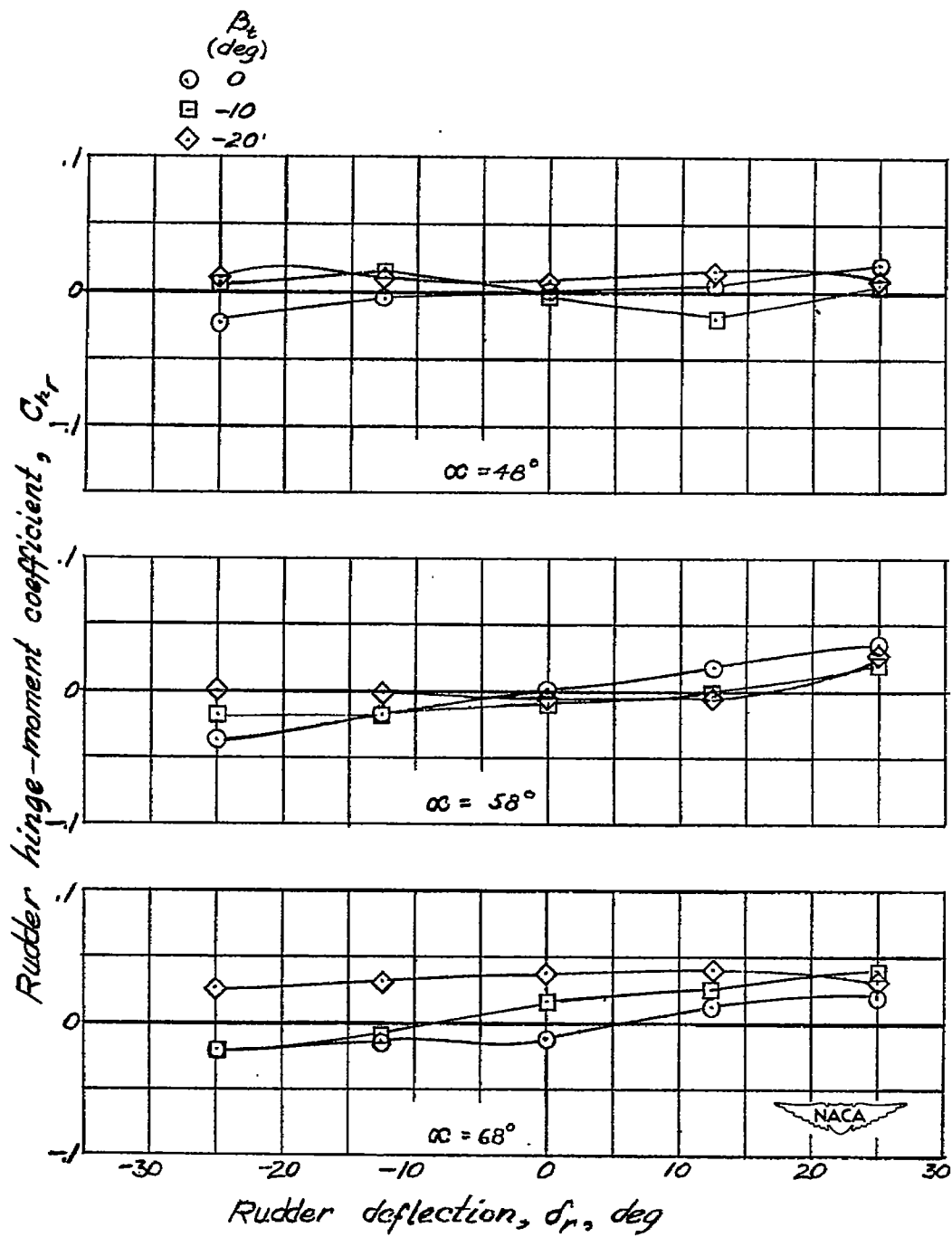
(b) Concluded. $\delta_e = 0°$.

Figure 10.— Continued.
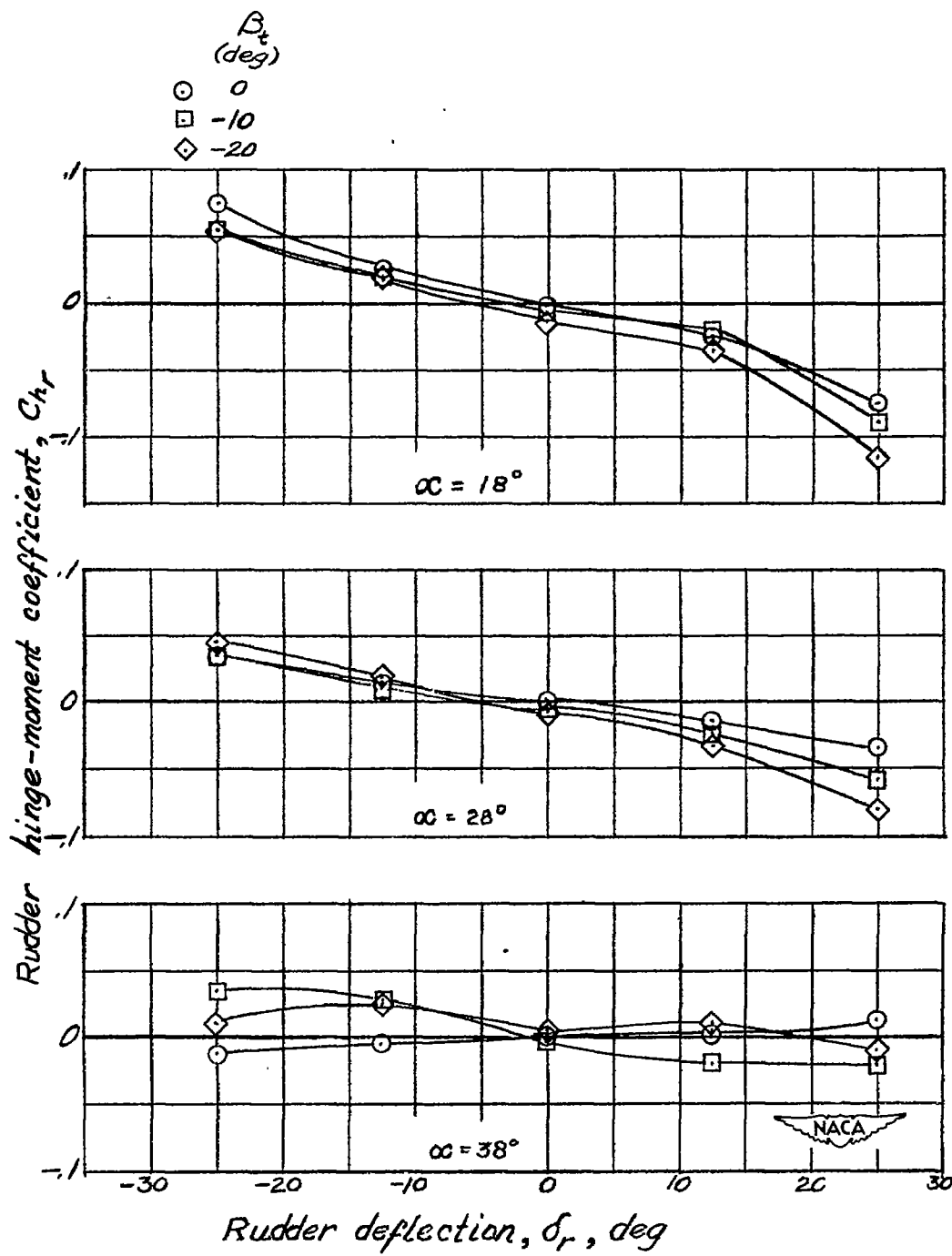
(c) $\delta_e = 20^\circ$.

Figure 10.— Continued.
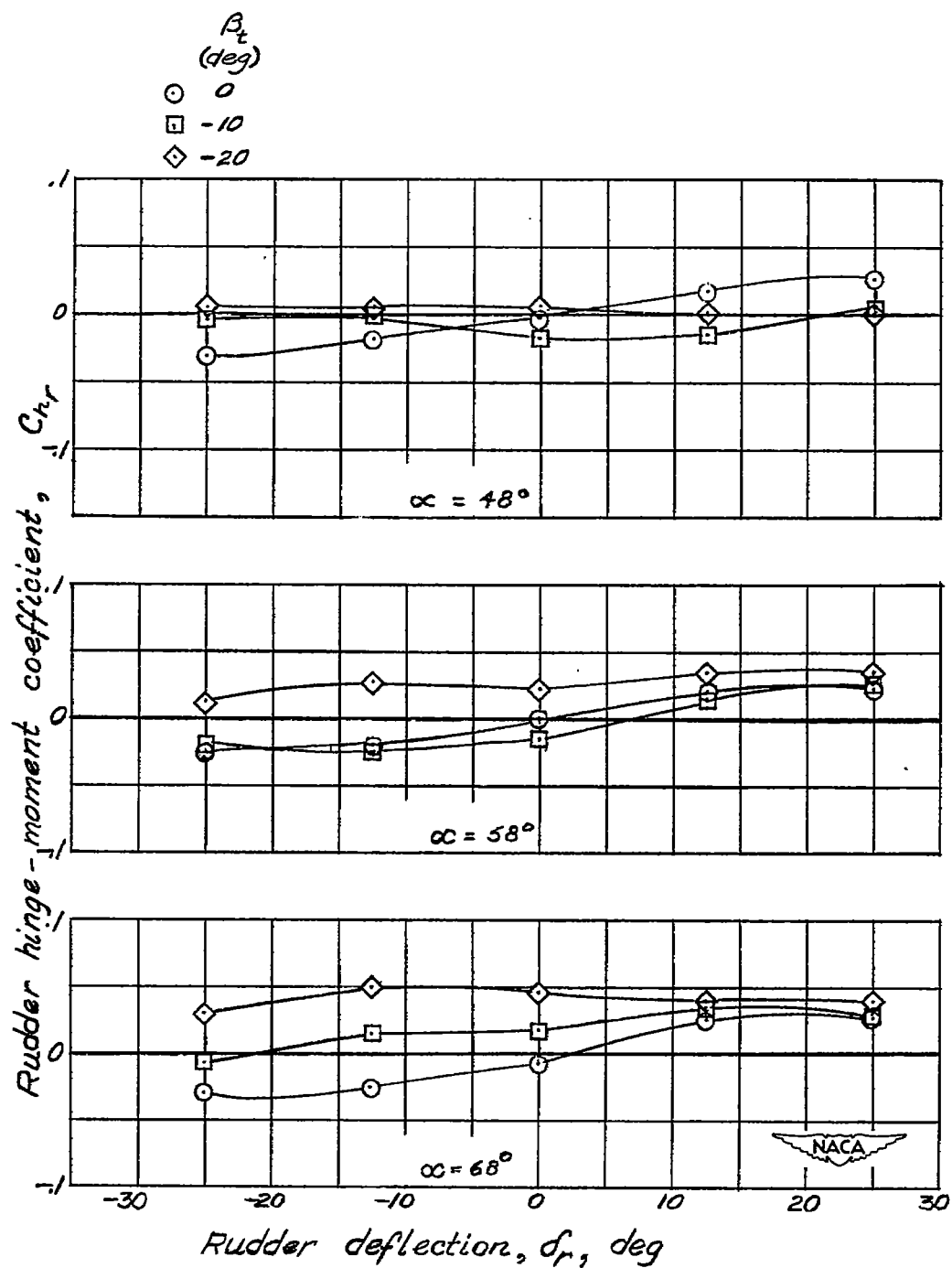
(c) Concluded. $\delta_e = 20^\circ$.

Figure 10.— Concluded.
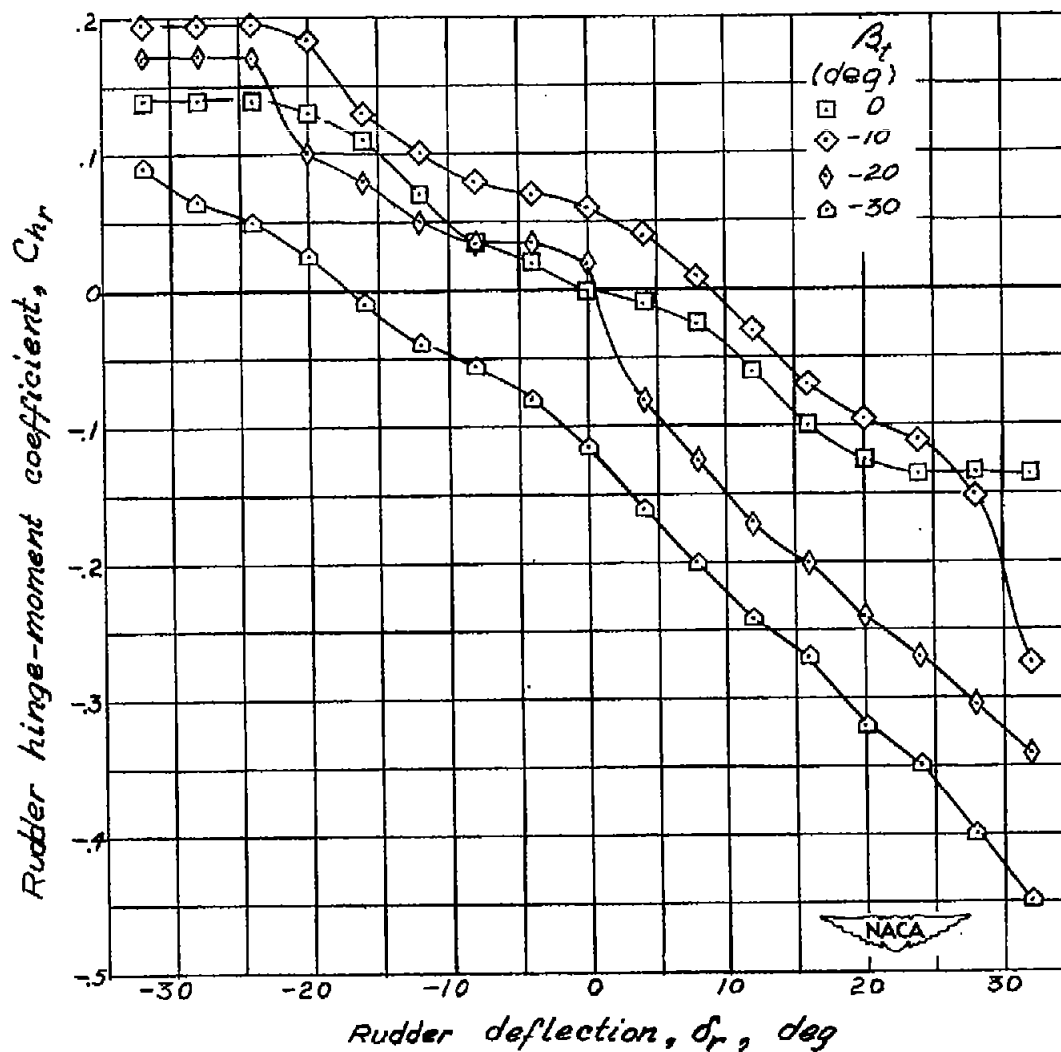
Figure 11.— Rudder hinge-moment coefficient as a function of rudder deflection at various angles of sideslip. 14.5-percent-horn-balanced rudder; α = 0°. Data from reference 9.
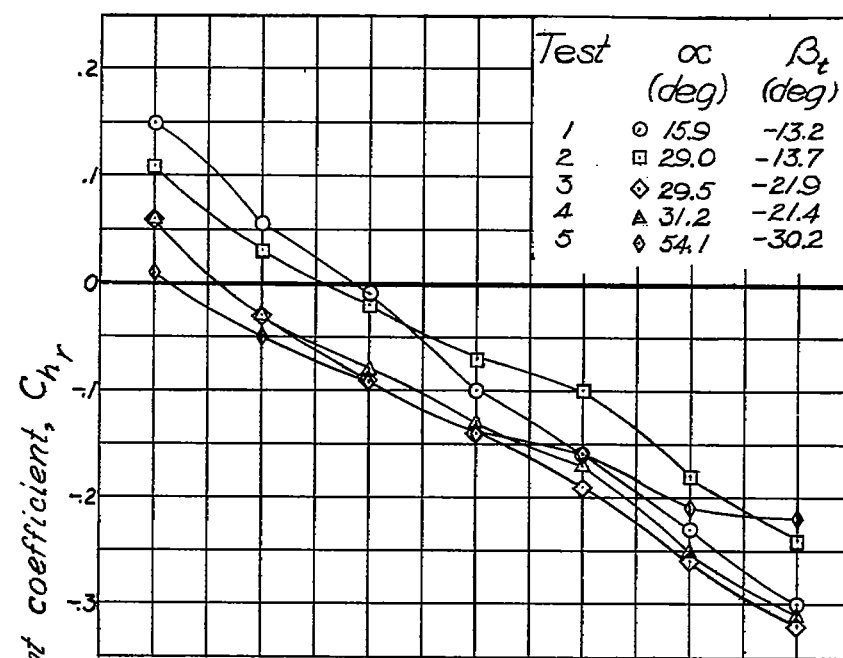
(a) Tail 1.
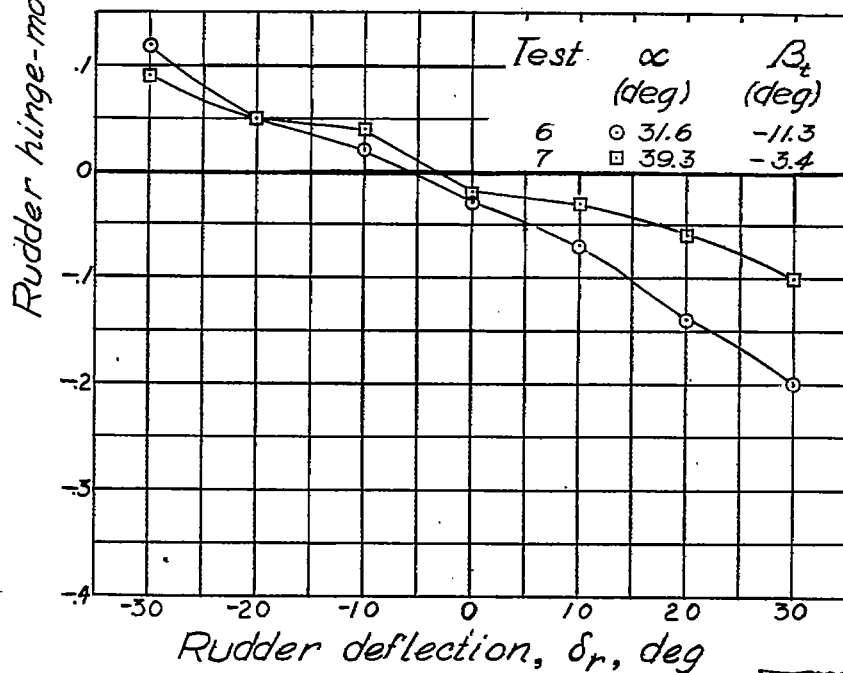
(b) Tail 2.

Figure 12.— Plain—rudder hinge—moment coefficient as a function of
rudder deflection at specific spinning attitudes. Normal—size
vertical and horizontal tails.

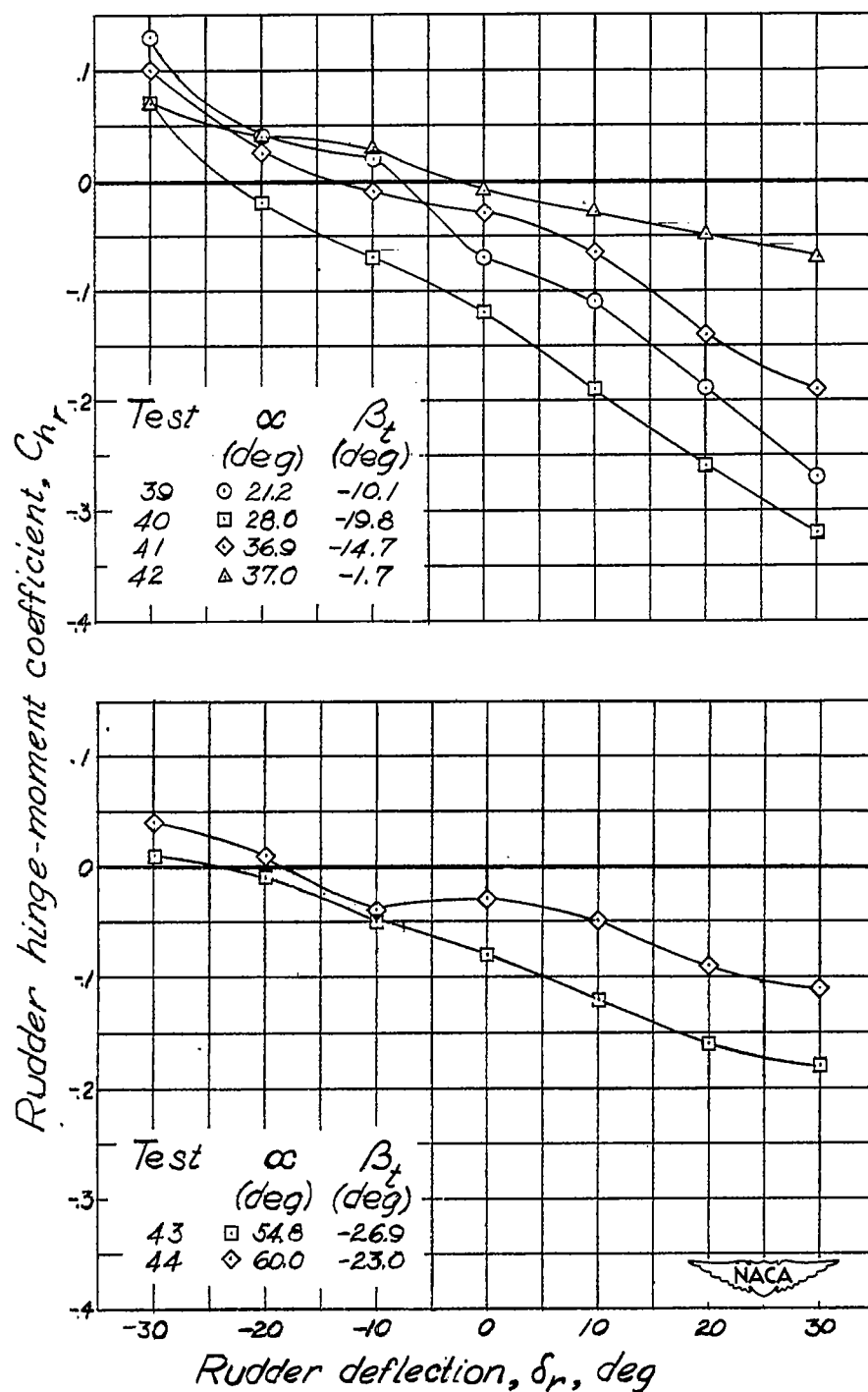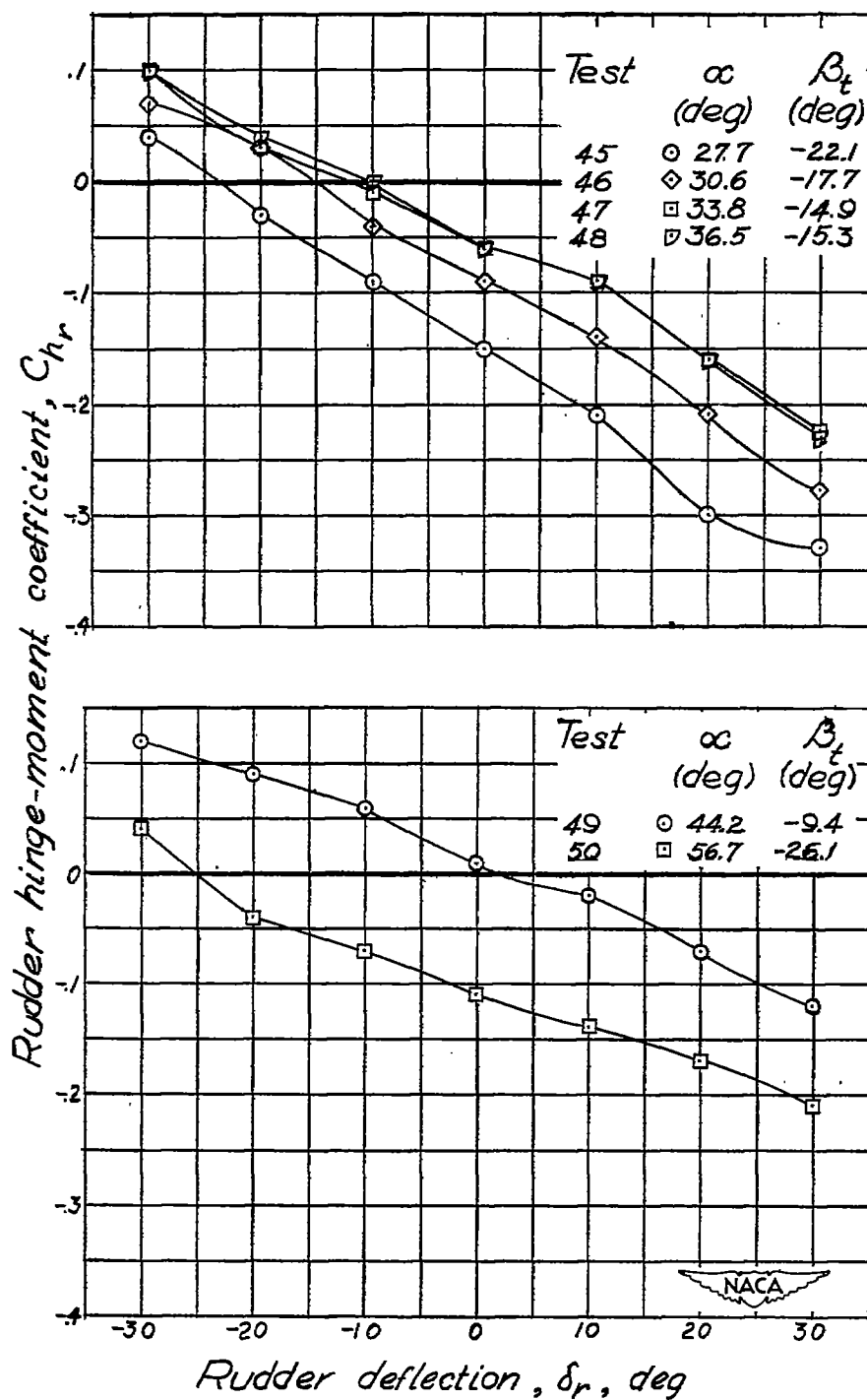| Test	α (deg)	β_t (deg)
8	⊙ 25.1	−20.0
9	⊡ 35.3	≠12.4
10	◇ 36.5	−22.1
11	▽ 42.9	− 9.6
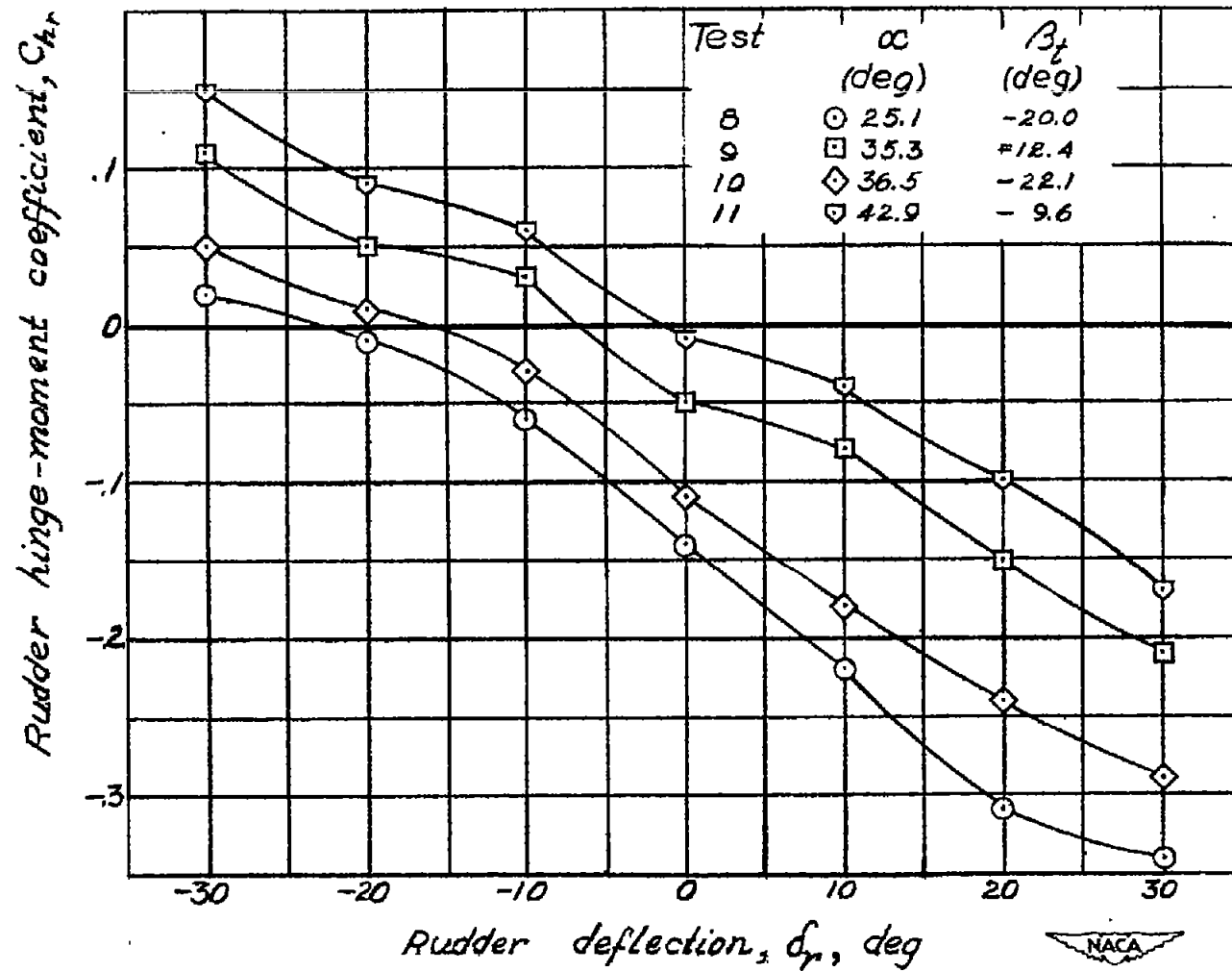
(c) Tail 3.

Figure 12.— Concluded.
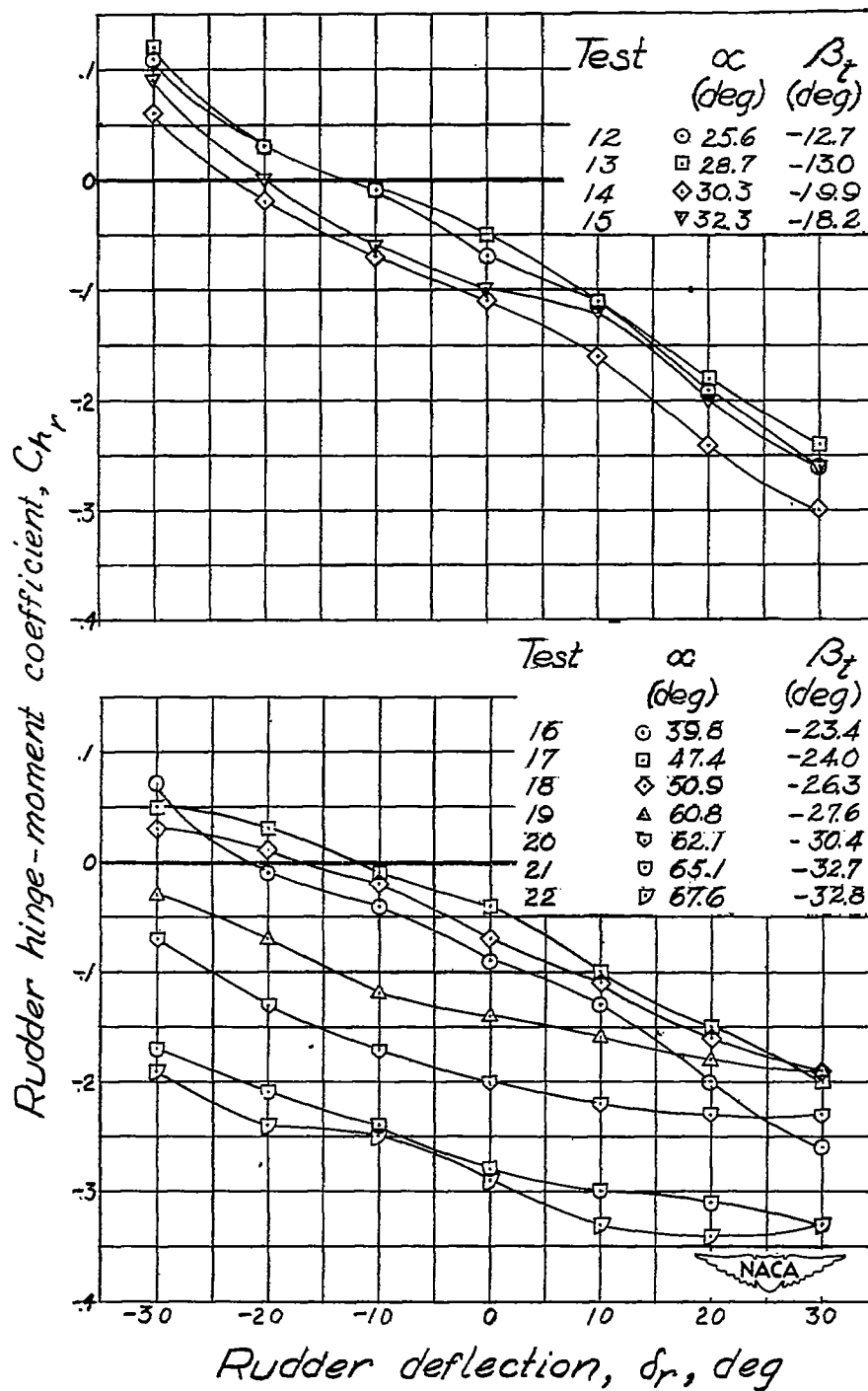
(a) Tail 4.

Figure 13.— Plain–rudder hinge–moment coefficient as a function of rudder
deflection at specific spinning attitudes. Normal–size vertical tail
and large–size horizontal tail.

Test	α (deg)	β_t (deg)
23	18.7	-9.2
24	28.4	-14.4
25	29.4	-10.9
26	33.5	-21.3
27	35.7	-21.2

Test	α (deg)	β_t (deg)
28	41.4	-23.6
29	53.8	-28.3
30	56.1	-28.5

Rudder hinge-moment coefficient, C_{h_r}

Rudder deflection, δ_r, deg
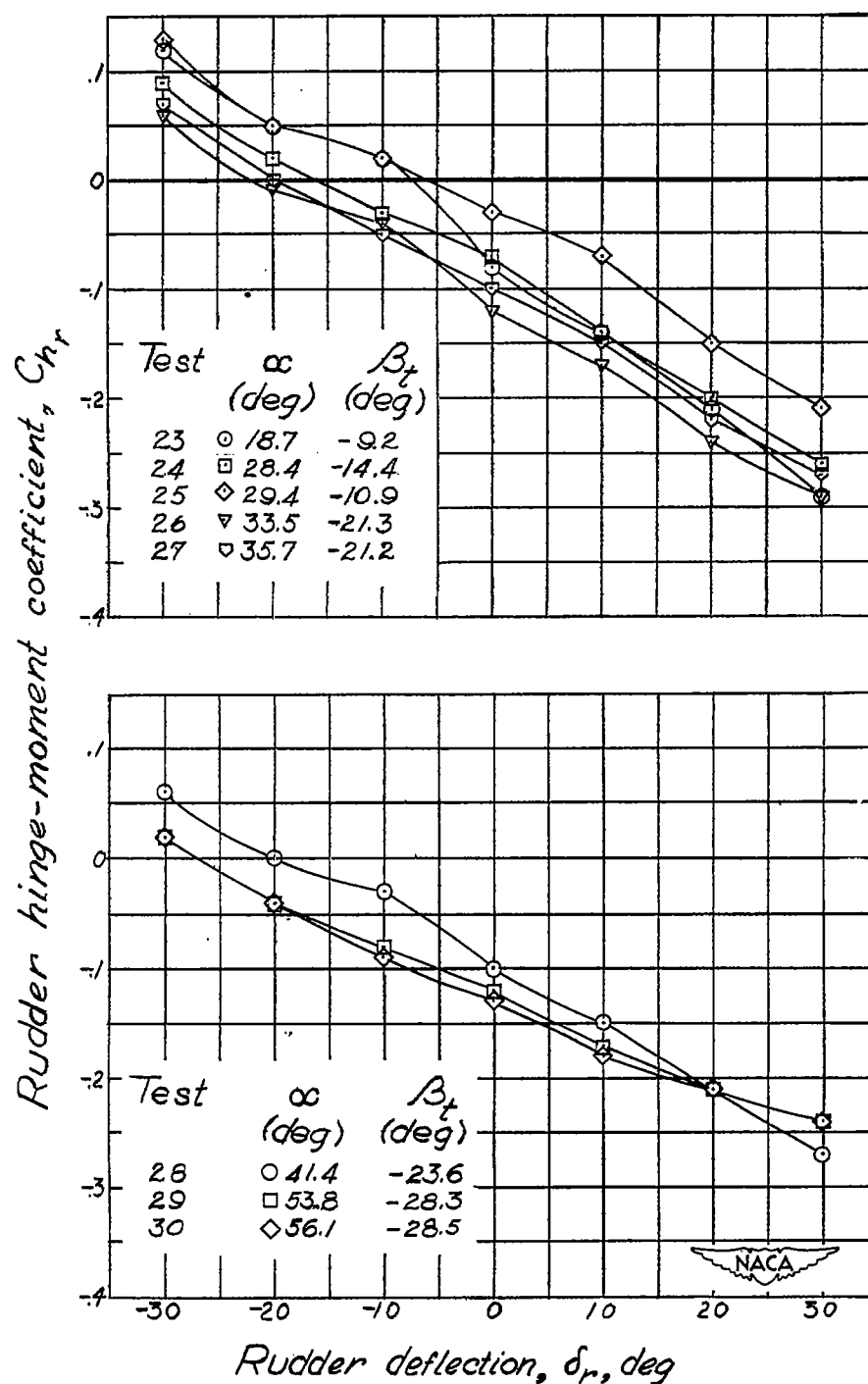
(b) Tail 5.

Figure 13.— Continued.

Top chart legend:

Test	α (deg)	β_t (deg)
31	27.7	-12.2
32	28.1	-16.7
33	29.0	-10.0
34	29.5	-13.2

Bottom chart legend:

Test	α (deg)	β_t (deg)
35	30.5	-2.2
36	30.8	-25.0
37	31.3	-2.5
38	34.6	-26.6

Rudder deflection, δ_r, deg

Rudder hinge-moment coefficient, C_{h_r}
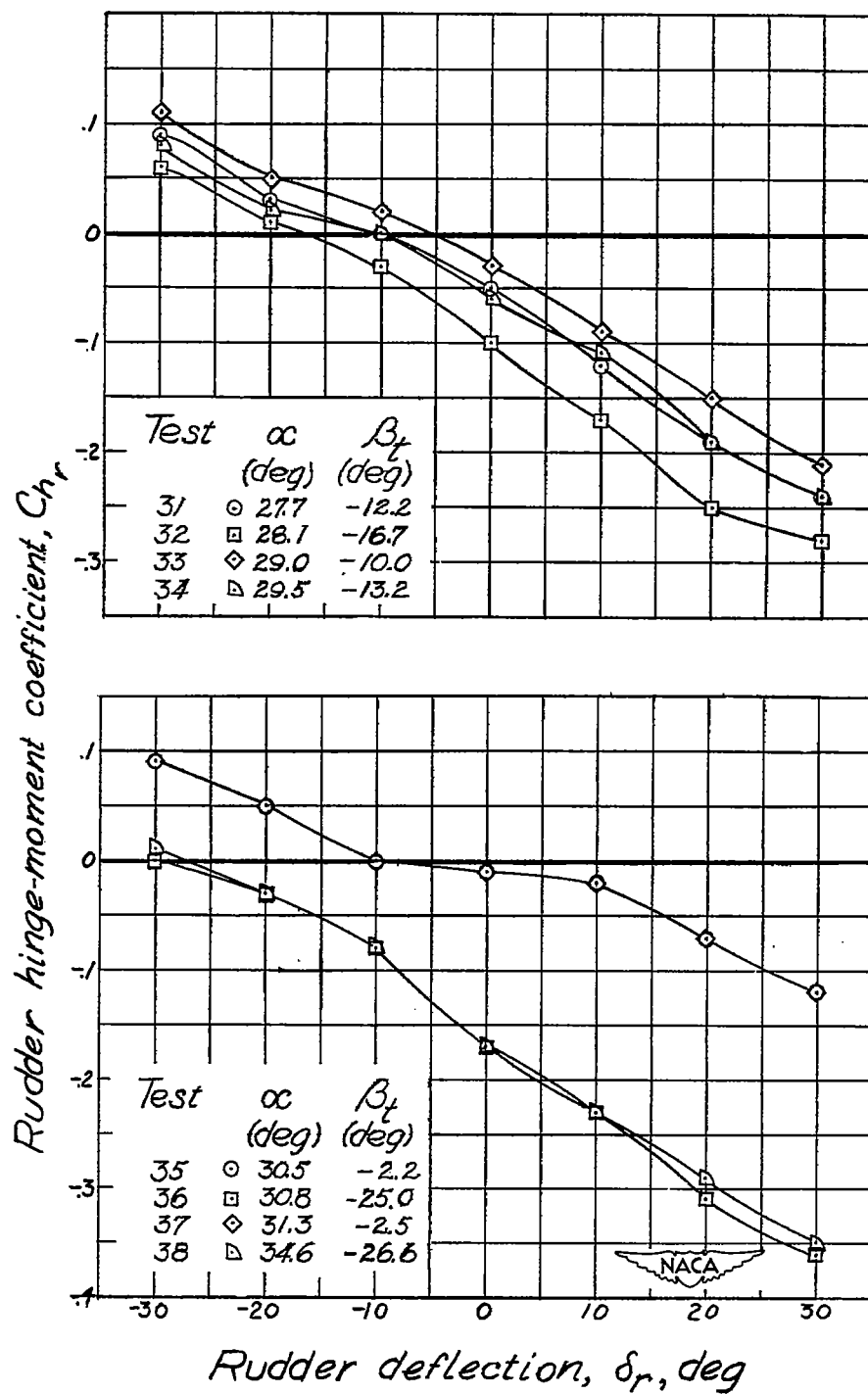
(c) Tail 6.

Figure 13.— Concluded.

(a) Tail 7.

Figure 14.— Plain-rudder hinge-moment coefficient as a function of rudder
   deflection at specific spinning attitudes. Large-size vertical tail
   and normal-size horizontal tail.

Test	α (deg)	β_t (deg)
45	⊙ 27.7	−22.1
46	◇ 30.6	−17.7
47	⊡ 33.8	−14.9
48	▽ 36.5	−15.3

Test	α (deg)	β_t (deg)
49	⊙ 44.2	−9.4
50	⊡ 56.7	−26.1

(b) Tail 8.

Figure 14.— Concluded.
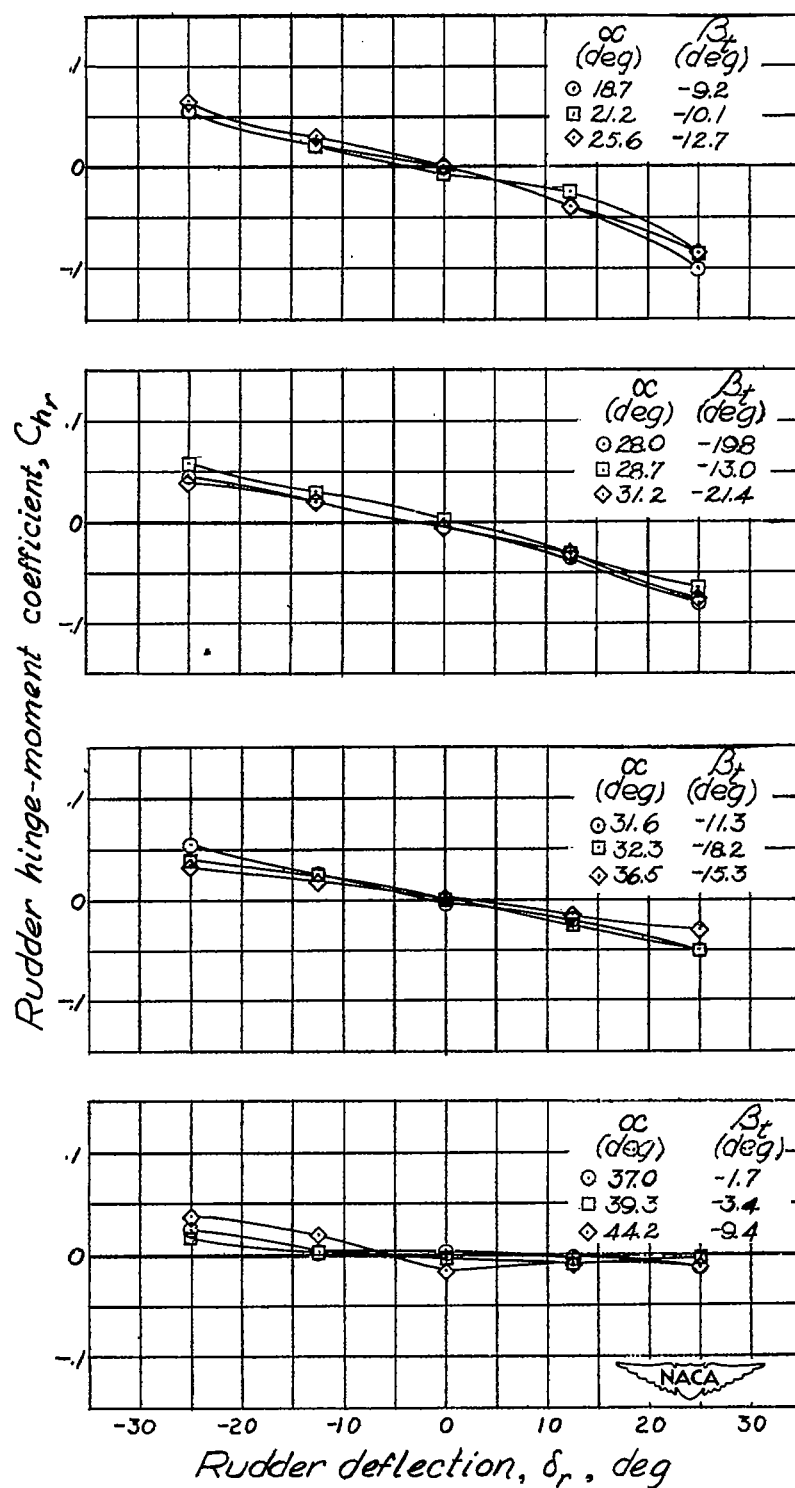
Figure 15.— Rudder hinge—moment coefficient as a function of rudder
deflection at specific spinning attitudes. 27.9—percent—overhang—
balanced rudder.
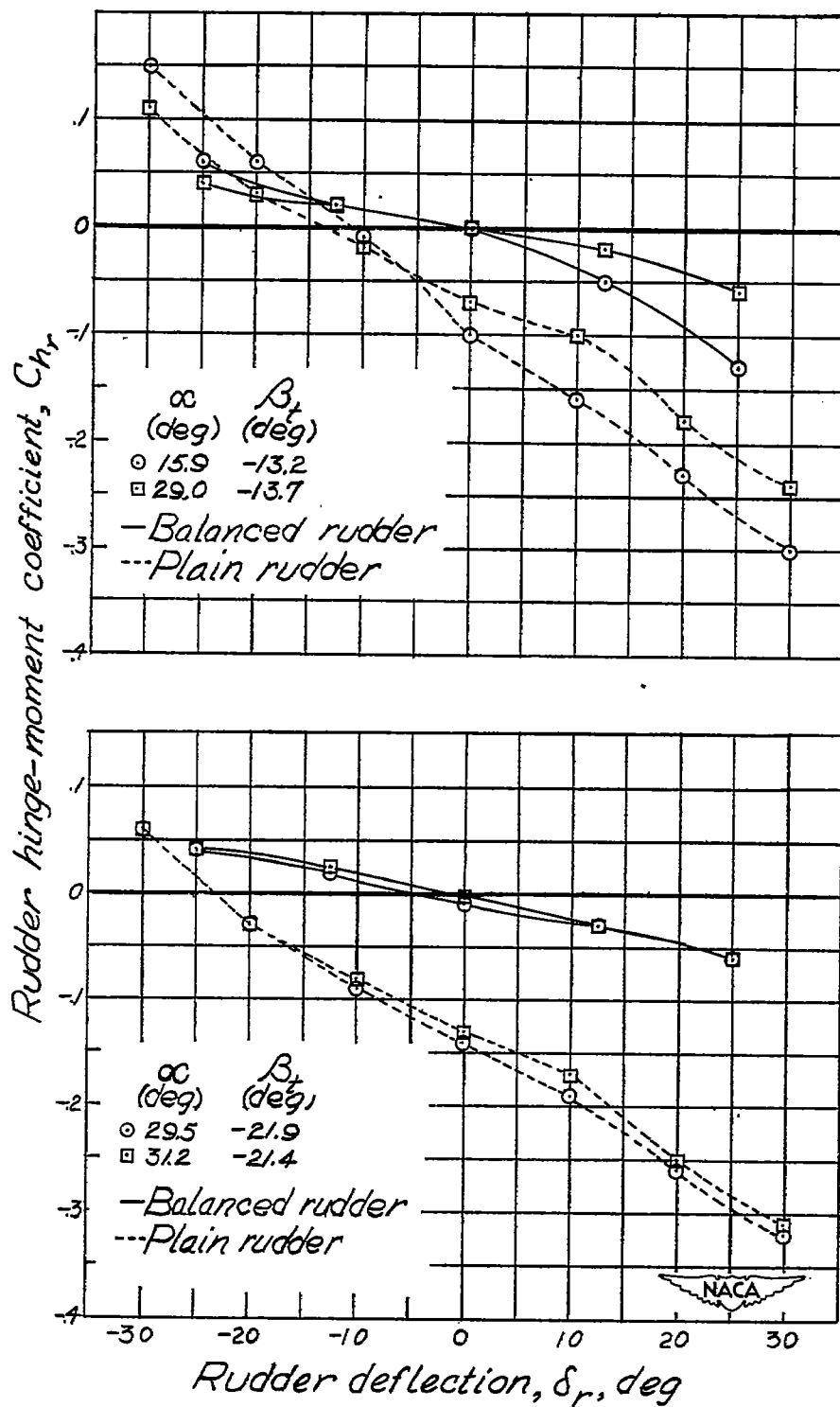
Figure 16.— Rudder hinge-moment coefficient as a function of rudder
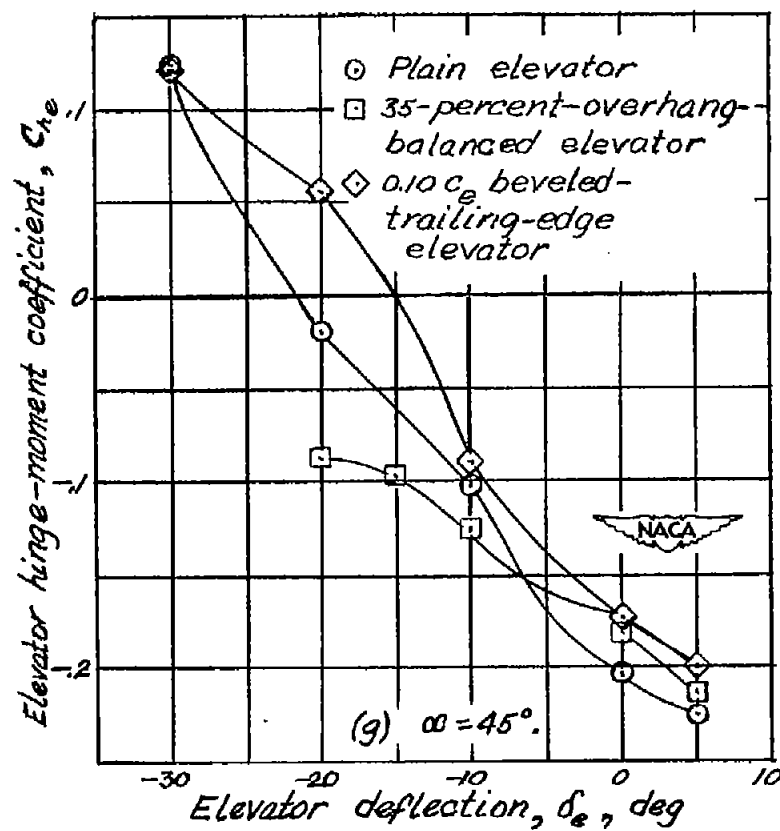deflection at various spinning attitudes for a 27.9-percent-overhang-
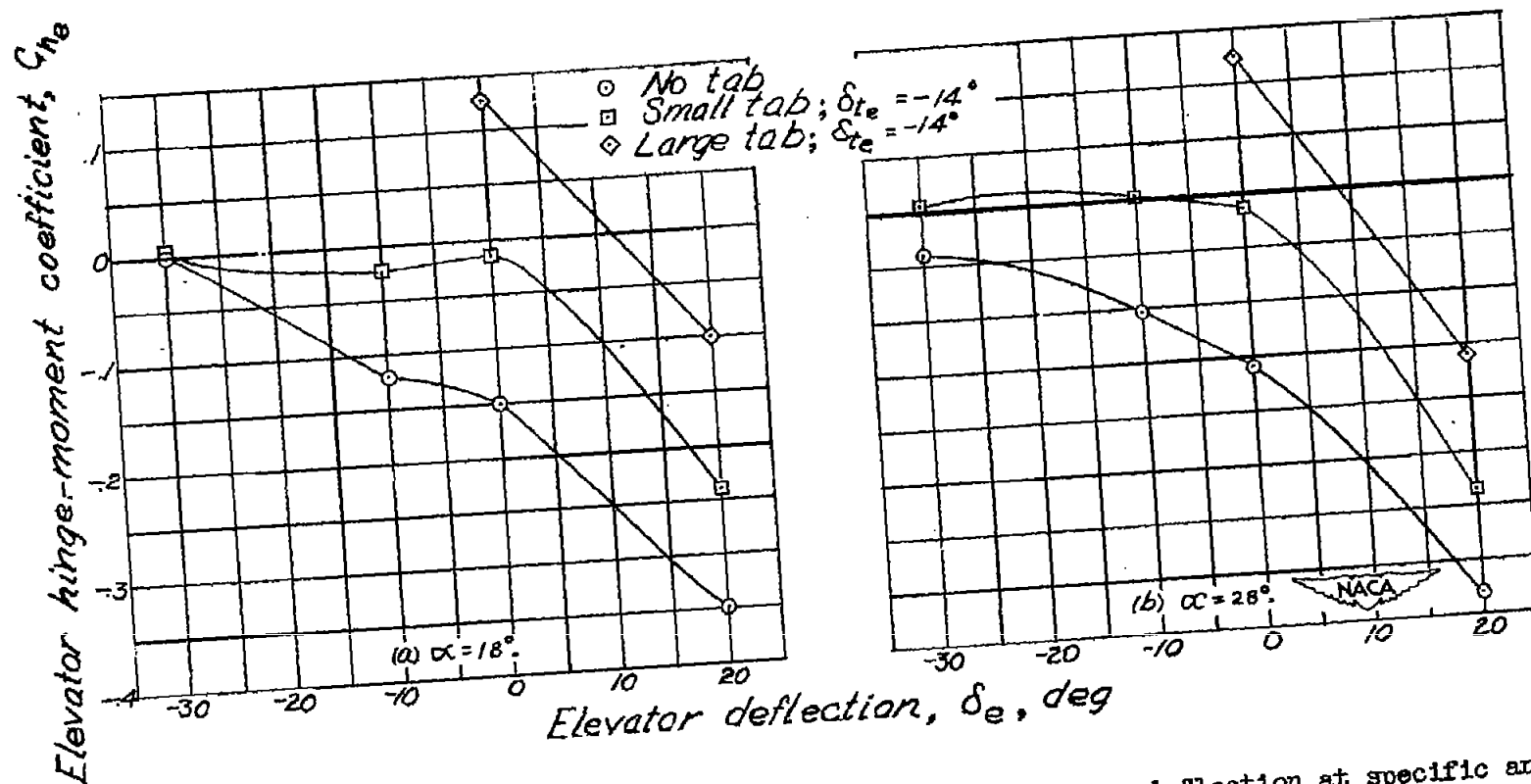balanced and a plain rudder.
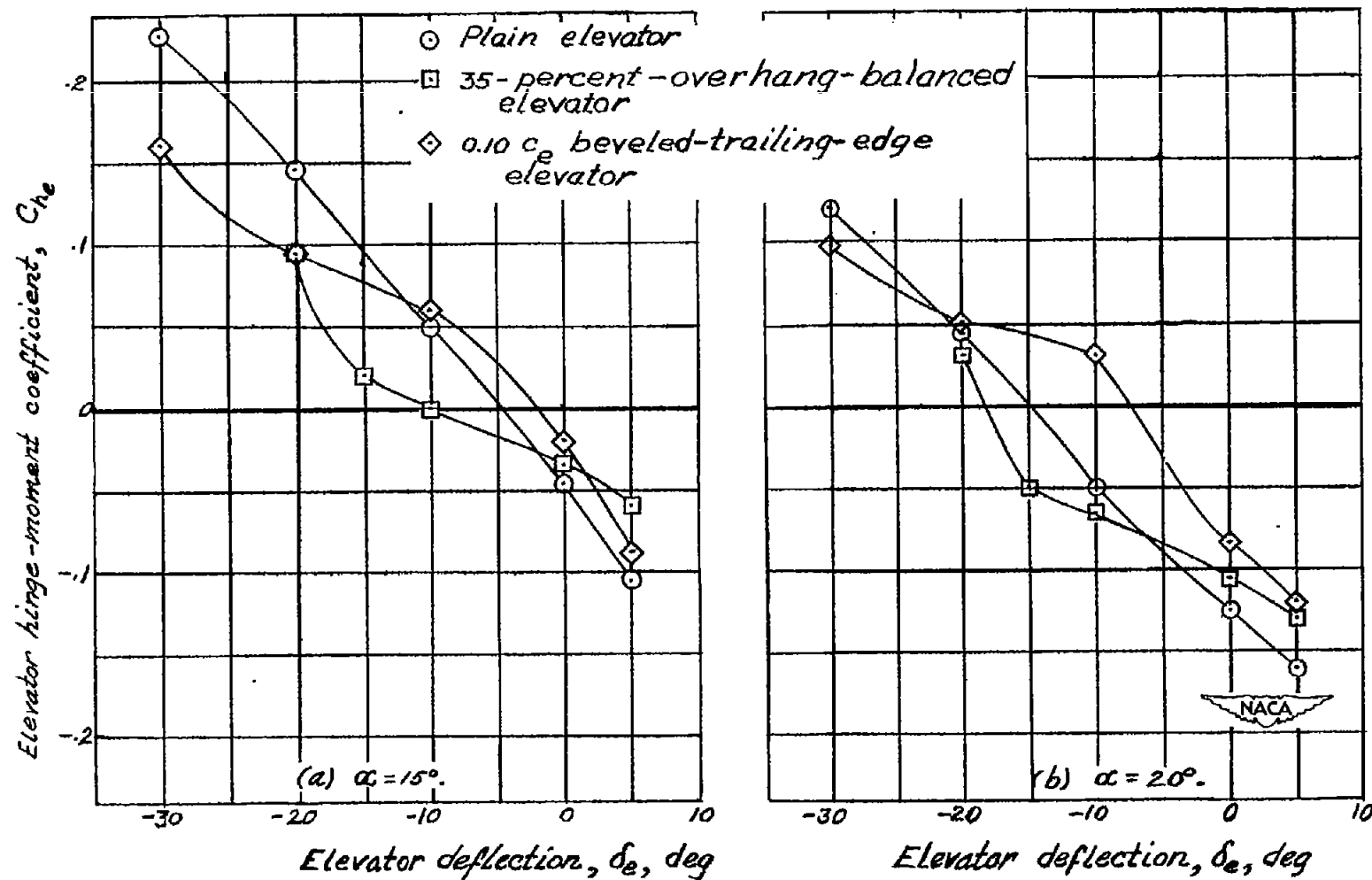
Figure 17.— Elevator hinge-moment coefficient as a function of elevator deflection at specific angles of attack for a plain and 35-percent-overhang-balanced elevator (reference 7) and a beveled-trailing-edge elevator (reference 8). $\beta_t = 0°$.
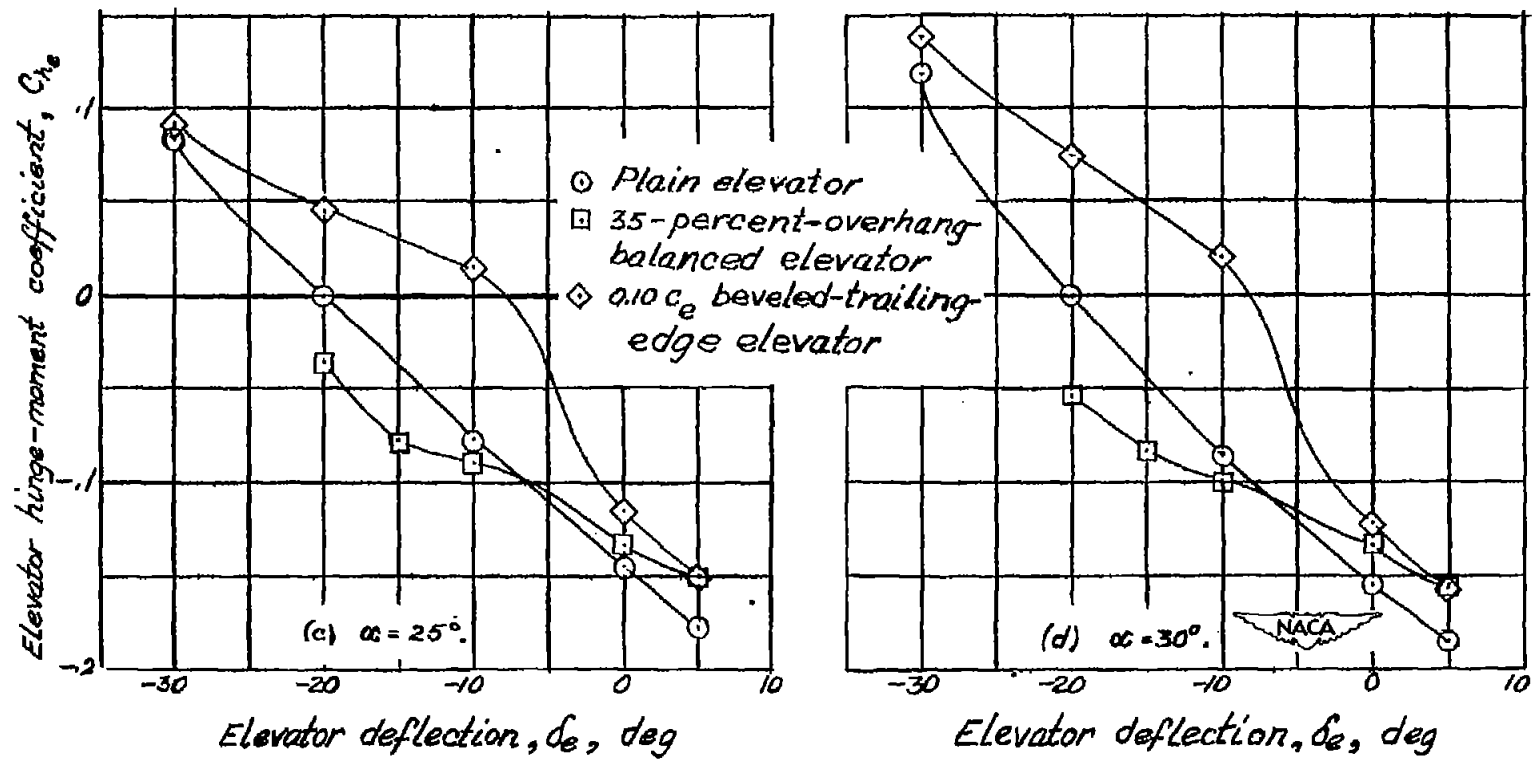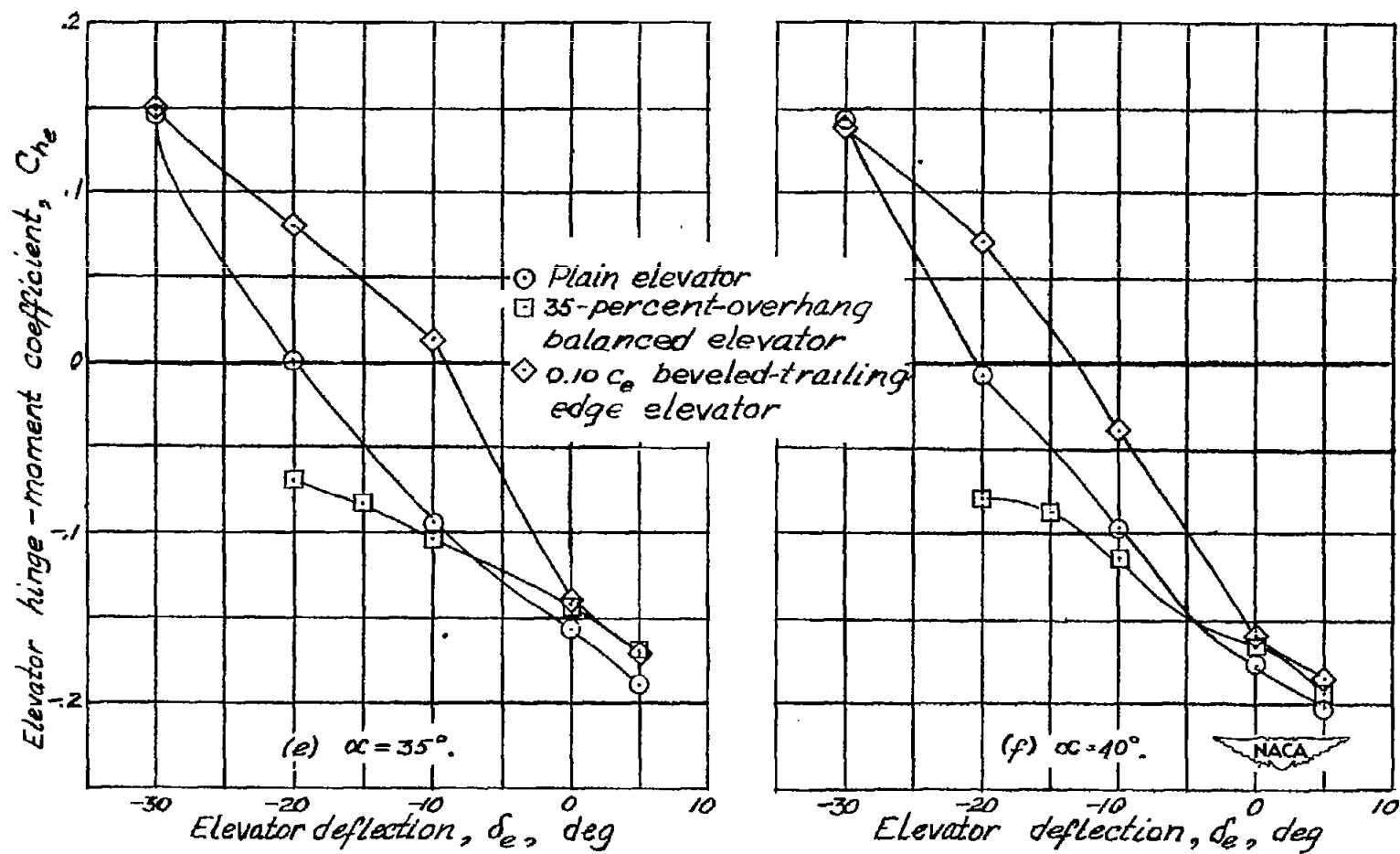
Figure 17.— Continued.

Figure 17.— Continued.

(g) $\alpha = 45°$.

Figure 17.— Concluded.

Figure 18.— Elevator hinge-moment coefficient as a function of elevator deflection at specific angles of attack for a 31.8-percent-overhang-balanced elevator with and without tabs deflected. $\beta_t = 0^\circ$. Data from reference 5.
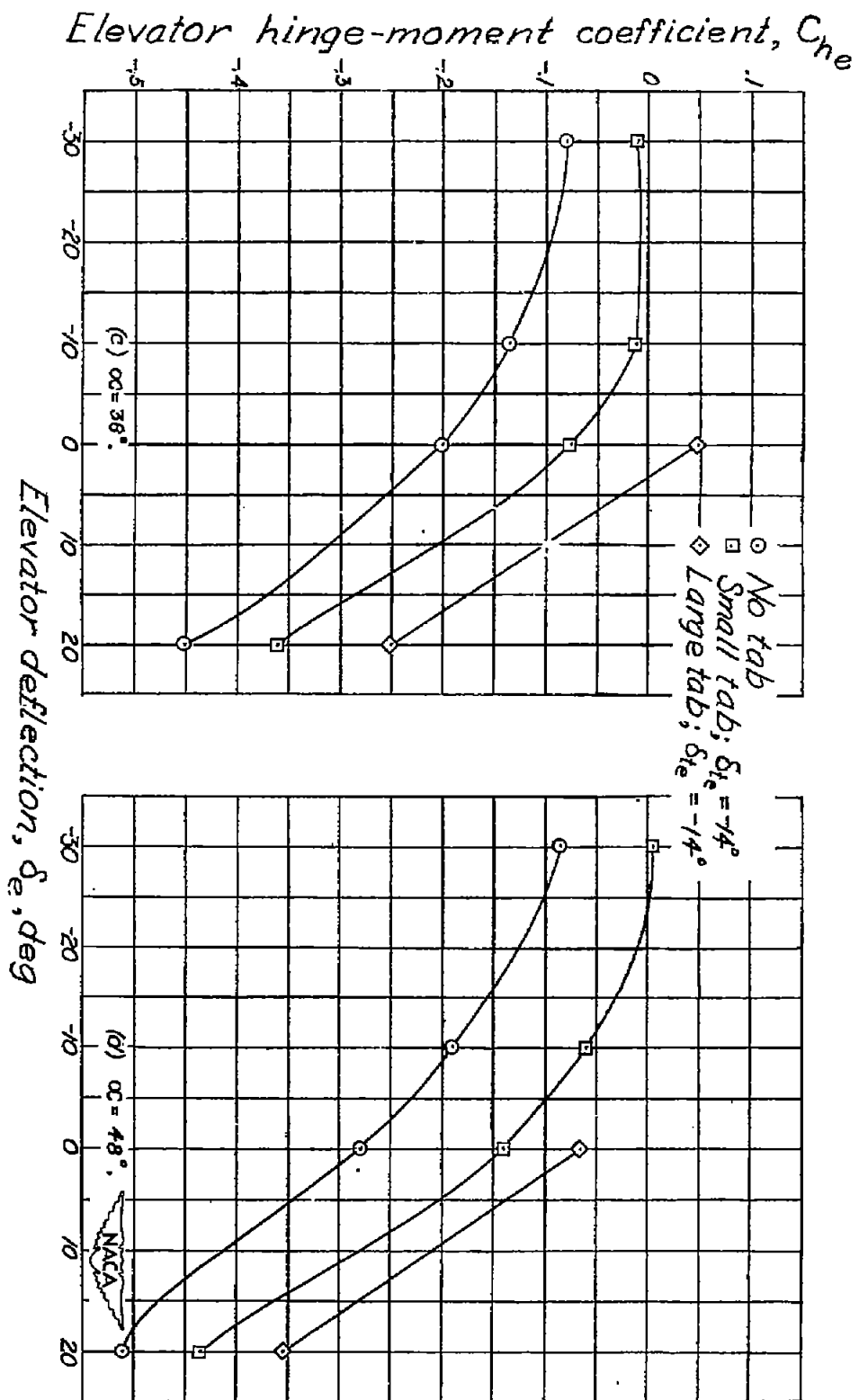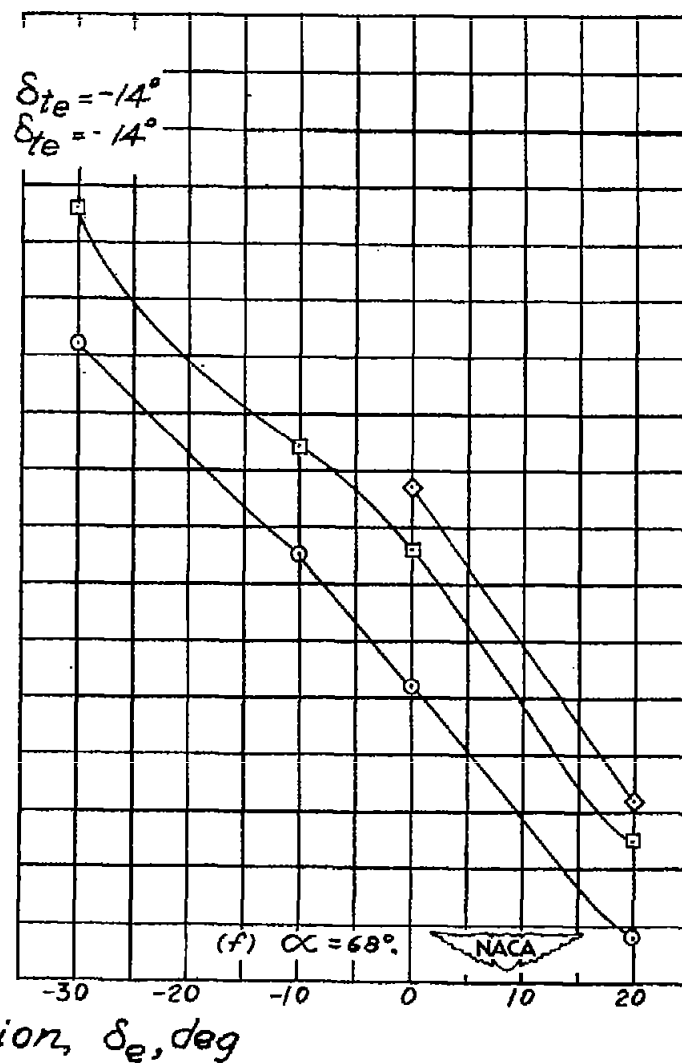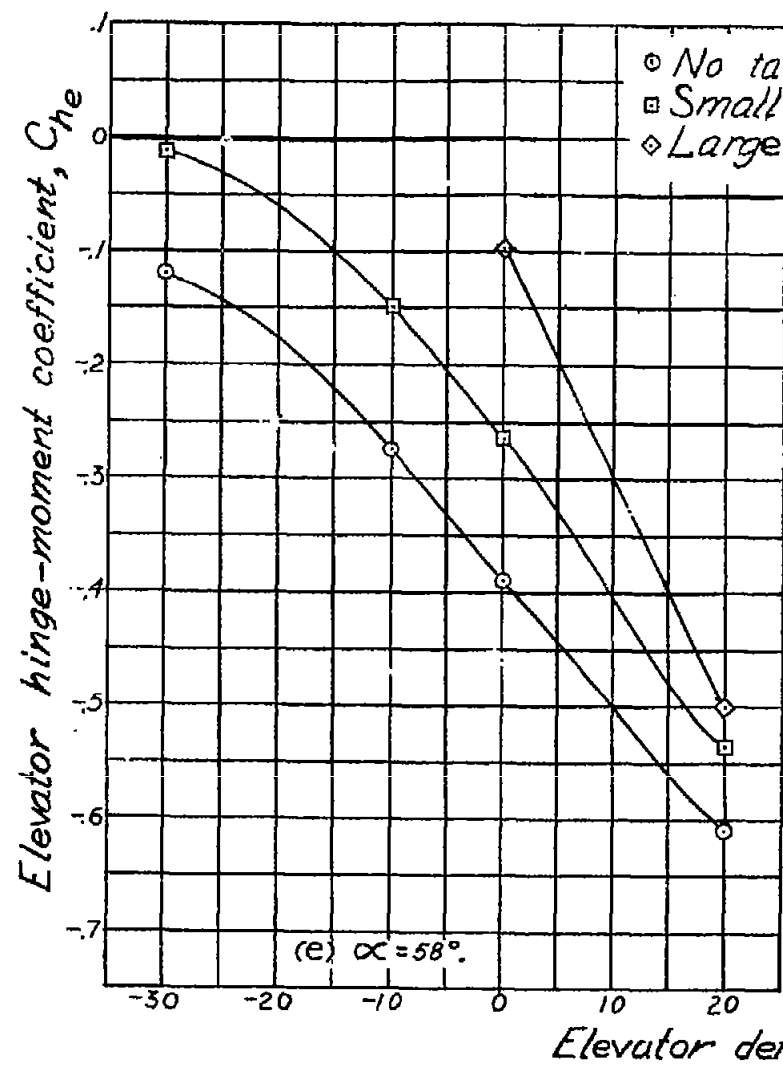
Figure 18.— Continued.

Figure 18.— Concluded.

Unshielded rudder area
Unshielded overhang balance area
Unshielded horn balance area

— Approximate wake for 30° angle of attack spin

--- Approximate wake for 45° angle of attack spin

60°

45°

30°

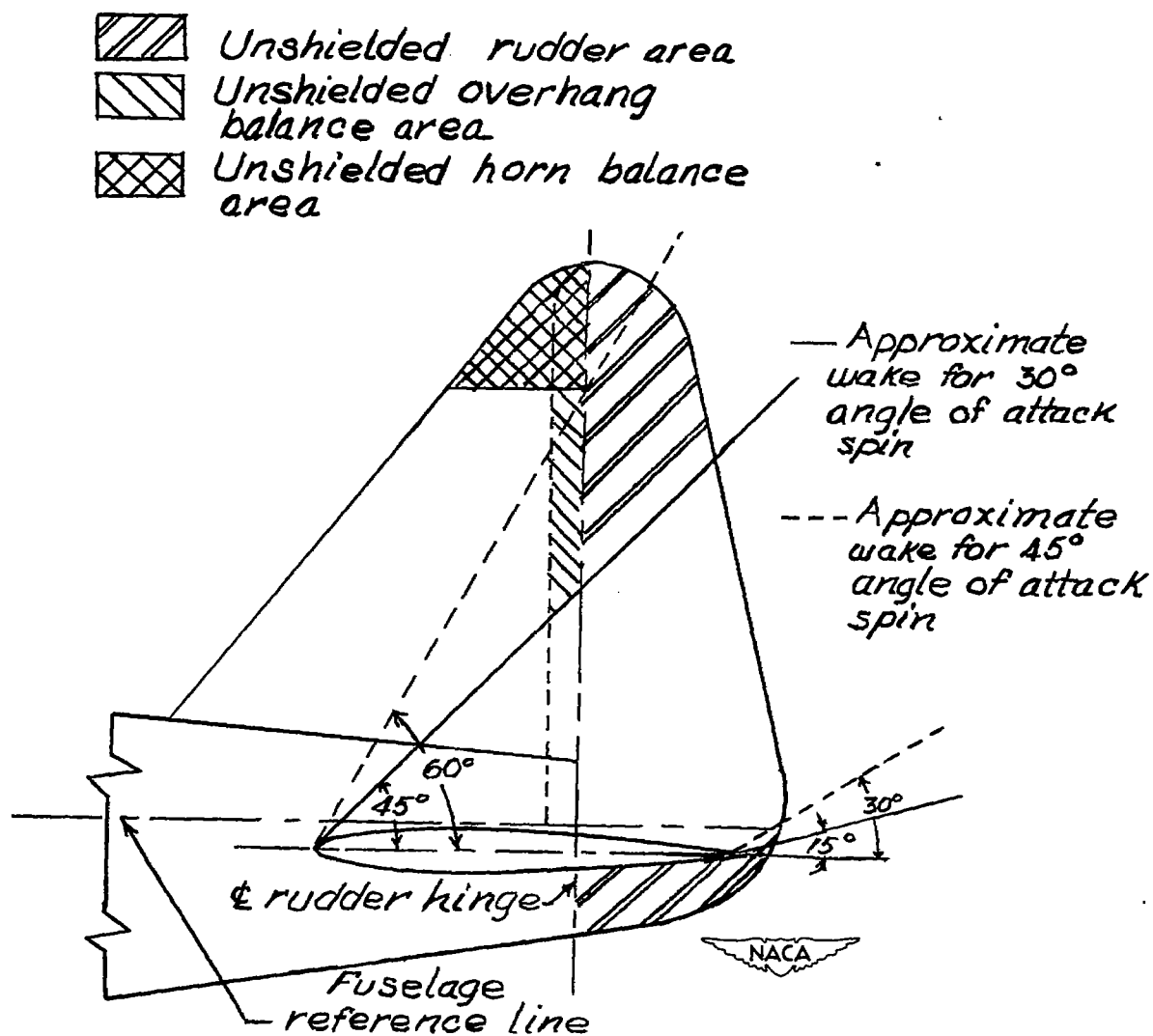15°

₵ rudder hinge

NACA

Fuselage reference line

Figure 19.— Sketch showing the shielding effect of the horizontal-tail wake on the vertical tail having an overhang-balanced or a horn-balanced rudder.